

## Supplementary Material

### **Novel asymmetric biscarbothioamides as Alzheimer's disease associated cholinesterase inhibitors: Synthesis, biological activity, and molecular docking studies**

Halit Muğlu <sup>a</sup>, Hasan Yakan <sup>b</sup>, Musa Erdoğan <sup>c,\*</sup>, Fevzi Topal <sup>d,\*</sup>, Meryem Topal <sup>e</sup>, Cüneyt Türkeş <sup>f</sup>, Şükrü Beydemir <sup>g,h</sup>

<sup>a</sup> *Department of Chemistry, Faculty of Sciences, Kastamonu University, Kastamonu 37200, Turkey*

<sup>b</sup> *Department of Chemistry Education, Faculty of Education, Ondokuz Mayıs University, Samsun 55200, Turkey*

<sup>c</sup> *Department of Food Engineering, Faculty of Engineering and Architecture, Kafkas University, Kars 36100, Turkey*

<sup>d</sup> *Department of Chemical and Chemical Processing Technologies, Laboratory Technology, Gümüşhane University, Gümüşhane 29100, Turkey*

<sup>e</sup> *Vocational School of Health Services, Gümüşhane University, Gümüşhane 29100, Turkey*

<sup>f</sup> *Department of Biochemistry, Faculty of Pharmacy, Erzincan Binali Yıldırım University, Erzincan 24002, Turkey*

<sup>g</sup> *Department of Biochemistry, Faculty of Pharmacy, Anadolu University, Eskişehir 26470, Turkey*

<sup>h</sup> *Bilecik Şeyh Edebalı University, Bilecik 11230, Turkey*

---

\* Corresponding authors.

Department of Food Engineering, Faculty of Engineering and Architecture, Kafkas University, Kars 36100, Turkey; E-mail: musa.erdogan@kafkas.edu.tr; ORCID ID: 0000-0001-6097-2862 (M.Erdoğan).

Department of Chemical and Chemical Processing Technologies, Laboratory Technology, Gümüşhane University, Gümüşhane 29100, Turkey; E-mail: ftopal@gumushane.edu.tr; ORCID ID: 0000-0002-2932-2789 (F.Topal).

## Table of Contents

- Table S1.** FT-IR values of the novel asymmetric bis(carbothioamides) (**3a-l**) ( $\text{cm}^{-1}$ ).
- Table S2.** ADME/T related parameters of the novel asymmetric bis(carbothioamides) (**3a-l**) and clinically used reference inhibitor tacrine.
- Table S3.** Pharmacokinetic properties of the novel asymmetric bis(carbothioamides) (**3a-l**) and clinically used reference inhibitor tacrine.
- Table S4.** Drug-likeness descriptors of the novel asymmetric bis(carbothioamides) (**3a-l**) and clinically used reference inhibitor tacrine.
- Table S5.** Medicinal Chemistry pattern recognition methods of the novel asymmetric bis(carbothioamides) (**3a-l**) and clinically used reference inhibitor tacrine.
- Fig. S1.** Diagrams showing 'drug-likeness' descriptors for the novel asymmetric bis(carbothioamides) (**3a-l**) and clinically used reference inhibitor tacrine. The red-colored zone has been identified as a feasible physicochemical domain to enhance oral bioavailability. LIPO, lipophilicity; SIZE, molecular weight; POLAR, polarity; INSOLU, insolubility; INSATU, saturation; and FLEX, flexibility.
- Fig. S2.**  $^1\text{H-NMR}$  (400 MHz,  $\text{DMSO-}d_6$ ) spectra of compound **3a** ( $N^1$ -ethyl- $N^2$ -phenylhydrazine-1,2-bis(carbothioamide)).
- Fig. S3.**  $^{13}\text{C-NMR}$  (100 MHz,  $\text{DMSO-}d_6$ ) spectra of compound **3a** ( $N^1$ -ethyl- $N^2$ -phenylhydrazine-1,2-bis(carbothioamide)).
- Fig. S4.** FT-IR spectra of compound **3a** ( $N^1$ -ethyl- $N^2$ -phenylhydrazine-1,2-bis(carbothioamide)).
- Fig. S5.** Lineweaver-Burk plots of compound **3a** ( $N^1$ -ethyl- $N^2$ -phenylhydrazine-1,2-bis(carbothioamide)).
- Fig. S6.**  $^1\text{H-NMR}$  (400 MHz,  $\text{DMSO-}d_6$ ) spectra of compound **3b** ( $N^1$ -(3-methoxyphenyl)- $N^2$ -phenylhydrazine-1,2-bis(carbothioamide)).
- Fig. S7.**  $^{13}\text{C-NMR}$  (100 MHz,  $\text{DMSO-}d_6$ ) spectra of compound **3b** ( $N^1$ -(3-methoxyphenyl)- $N^2$ -phenylhydrazine-1,2-bis(carbothioamide)).
- Fig. S8.** FT-IR spectra of compound **3b** ( $N^1$ -(3-methoxyphenyl)- $N^2$ -phenylhydrazine-1,2-bis(carbothioamide)).
- Fig. S9.** Lineweaver-Burk plots of compound **3b** ( $N^1$ -(3-methoxyphenyl)- $N^2$ -phenylhydrazine-1,2-bis(carbothioamide)).
- Fig. S10.**  $^1\text{H-NMR}$  (400 MHz,  $\text{DMSO-}d_6$ ) spectra of compound **3c** ( $N^1$ -(4-methoxyphenyl)- $N^2$ -phenylhydrazine-1,2-bis(carbothioamide)).
- Fig. S11.**  $^{13}\text{C-NMR}$  (100 MHz,  $\text{DMSO-}d_6$ ) spectra of compound **3c** ( $N^1$ -(4-methoxyphenyl)- $N^2$ -phenylhydrazine-1,2-bis(carbothioamide)).
- Fig. S12.** FT-IR spectra of compound **3c** ( $N^1$ -(4-methoxyphenyl)- $N^2$ -phenylhydrazine-1,2-bis(carbothioamide)).
- Fig. S13.** Lineweaver-Burk plots of compound **3c** ( $N^1$ -(4-methoxyphenyl)- $N^2$ -phenylhydrazine-1,2-bis(carbothioamide)).
- Fig. S14.**  $^1\text{H-NMR}$  (400 MHz,  $\text{DMSO-}d_6$ ) spectra of compound **3d** ( $N^1$ -(4-chlorophenyl)- $N^2$ -phenylhydrazine-1,2-bis(carbothioamide)).

- Fig. S15.**  $^{13}\text{C}$ -NMR (100 MHz,  $\text{DMSO-}d_6$ ) spectra of compound **3d** ( $N^1$ -(4-chlorophenyl)- $N^2$ -phenylhydrazine-1,2-bis(carbothioamide)).
- Fig. S16.** FT-IR spectra of compound **3d** ( $N^1$ -(4-chlorophenyl)- $N^2$ -phenylhydrazine-1,2-bis(carbothioamide)).
- Fig. S17.** Lineweaver-Burk plots of compound **3d** ( $N^1$ -(4-chlorophenyl)- $N^2$ -phenylhydrazine-1,2-bis(carbothioamide)).
- Fig. S18.**  $^1\text{H}$ -NMR (400 MHz,  $\text{DMSO-}d_6$ ) spectra of compound **3e** ( $N^1$ -(2-fluorophenyl)- $N^2$ -phenylhydrazine-1,2-bis(carbothioamide)).
- Fig. S19.**  $^{13}\text{C}$ -NMR (100 MHz,  $\text{DMSO-}d_6$ ) spectra of compound **3e** ( $N^1$ -(2-fluorophenyl)- $N^2$ -phenylhydrazine-1,2-bis(carbothioamide)).
- Fig. S20.** FT-IR spectra of compound **3e** ( $N^1$ -(2-fluorophenyl)- $N^2$ -phenylhydrazine-1,2-bis(carbothioamide)).
- Fig. S21.** Lineweaver-Burk plots of compound **3e** ( $N^1$ -(2-fluorophenyl)- $N^2$ -phenylhydrazine-1,2-bis(carbothioamide)).
- Fig. S22.**  $^1\text{H}$ -NMR (400 MHz,  $\text{DMSO-}d_6$ ) spectra of compound **3f** ( $N^1$ -phenyl- $N^2$ -(*p*-tolyl)hydrazine-1,2-bis(carbothioamide)).
- Fig. S23.**  $^{13}\text{C}$ -NMR (100 MHz,  $\text{DMSO-}d_6$ ) spectra of compound **3f** ( $N^1$ -phenyl- $N^2$ -(*p*-tolyl)hydrazine-1,2-bis(carbothioamide)).
- Fig. S24.** FT-IR spectra of compound **3f** ( $N^1$ -phenyl- $N^2$ -(*p*-tolyl)hydrazine-1,2-bis(carbothioamide)).
- Fig. S25.** Lineweaver-Burk plots of compound **3f** ( $N^1$ -phenyl- $N^2$ -(*p*-tolyl)hydrazine-1,2-bis(carbothioamide)).
- Fig. S26.**  $^1\text{H}$ -NMR (400 MHz,  $\text{DMSO-}d_6$ ) spectra of compound **3g** ( $N^1$ -allyl- $N^2$ -(4-nitrophenyl)hydrazine-1,2-bis(carbothioamide)).
- Fig. S27.**  $^{13}\text{C}$ -NMR (100 MHz,  $\text{DMSO-}d_6$ ) spectra of compound **3g** ( $N^1$ -allyl- $N^2$ -(4-nitrophenyl)hydrazine-1,2-bis(carbothioamide)).
- Fig. S28.** FT-IR spectra of compound **3g** ( $N^1$ -allyl- $N^2$ -(4-nitrophenyl)hydrazine-1,2-bis(carbothioamide)).
- Fig. S29.** Lineweaver-Burk plots of compound **3g** ( $N^1$ -allyl- $N^2$ -(4-nitrophenyl)hydrazine-1,2-bis(carbothioamide)).
- Fig. S30.**  $^1\text{H}$ -NMR (400 MHz,  $\text{DMSO-}d_6$ ) spectra of compound **3h** ( $N^1$ -(3-methoxyphenyl)- $N^2$ -(4-nitrophenyl)hydrazine-1,2-bis(carbothioamide)).
- Fig. S31.**  $^{13}\text{C}$ -NMR (100 MHz,  $\text{DMSO-}d_6$ ) spectra of compound **3h** ( $N^1$ -(3-methoxyphenyl)- $N^2$ -(4-nitrophenyl)hydrazine-1,2-bis(carbothioamide)).
- Fig. S32.** FT-IR spectra of compound **3h** ( $N^1$ -(3-methoxyphenyl)- $N^2$ -(4-nitrophenyl)hydrazine-1,2-bis(carbothioamide)).
- Fig. S33.** Lineweaver-Burk plots of compound **3h** ( $N^1$ -(3-methoxyphenyl)- $N^2$ -(4-nitrophenyl)hydrazine-1,2-bis(carbothioamide)).
- Fig. S34.**  $^1\text{H}$ -NMR (400 MHz,  $\text{DMSO-}d_6$ ) spectra of compound **3i** ( $N^1$ -(4-methoxyphenyl)- $N^2$ -(4-nitrophenyl)hydrazine-1,2-bis(carbothioamide)).
- Fig. S35.**  $^{13}\text{C}$ -NMR (100 MHz,  $\text{DMSO-}d_6$ ) spectra of compound **3i** ( $N^1$ -(4-methoxyphenyl)- $N^2$ -(4-nitrophenyl)hydrazine-1,2-bis(carbothioamide)).

- Fig. S36.** FT-IR spectra of compound **3i** (*N*<sup>1</sup>-(4-methoxyphenyl)-*N*<sup>2</sup>-(4-nitrophenyl)hydrazine-1,2-bis(carbothioamide)).
- Fig. S37.** Lineweaver-Burk plots of compound **3i** (*N*<sup>1</sup>-(4-methoxyphenyl)-*N*<sup>2</sup>-(4-nitrophenyl)hydrazine-1,2-bis(carbothioamide)).
- Fig. S38.** <sup>1</sup>H-NMR (400 MHz, DMSO-*d*<sub>6</sub>) spectra of compound **3j** (*N*<sup>1</sup>-(3-fluorophenyl)-*N*<sup>2</sup>-(4-nitrophenyl)hydrazine-1,2-bis(carbothioamide)).
- Fig. S39.** <sup>13</sup>C-NMR (100 MHz, DMSO-*d*<sub>6</sub>) spectra of compound **3j** (*N*<sup>1</sup>-(3-fluorophenyl)-*N*<sup>2</sup>-(4-nitrophenyl)hydrazine-1,2-bis(carbothioamide)).
- Fig. S40.** FT-IR spectra of compound **3j** (*N*<sup>1</sup>-(3-fluorophenyl)-*N*<sup>2</sup>-(4-nitrophenyl)hydrazine-1,2-bis(carbothioamide)).
- Fig. S41.** Lineweaver-Burk plots of compound **3j** (*N*<sup>1</sup>-(3-fluorophenyl)-*N*<sup>2</sup>-(4-nitrophenyl)hydrazine-1,2-bis(carbothioamide)).
- Fig. S42.** <sup>1</sup>H-NMR (400 MHz, DMSO-*d*<sub>6</sub>) spectra of compound **3k** (*N*<sup>1</sup>-benzyl-*N*<sup>2</sup>-(4-nitrophenyl)hydrazine-1,2-bis(carbothioamide)).
- Fig. S43.** <sup>13</sup>C-NMR (100 MHz, DMSO-*d*<sub>6</sub>) spectra of compound **3k** (*N*<sup>1</sup>-benzyl-*N*<sup>2</sup>-(4-nitrophenyl)hydrazine-1,2-bis(carbothioamide)).
- Fig. S44.** FT-IR spectra of compound **3k** (*N*<sup>1</sup>-benzyl-*N*<sup>2</sup>-(4-nitrophenyl)hydrazine-1,2-bis(carbothioamide)).
- Fig. S45.** Lineweaver-Burk plots of compound **3k** (*N*<sup>1</sup>-benzyl-*N*<sup>2</sup>-(4-nitrophenyl)hydrazine-1,2-bis(carbothioamide)).
- Fig. S46.** <sup>1</sup>H-NMR (400 MHz, DMSO-*d*<sub>6</sub>) spectra of compound **3l** (*N*<sup>1</sup>-(3-chlorophenyl)-*N*<sup>2</sup>-(4-nitrophenyl)hydrazine-1,2-bis(carbothioamide)).
- Fig. S47.** <sup>13</sup>C-NMR (100 MHz, DMSO-*d*<sub>6</sub>) spectra of compound **3l** (*N*<sup>1</sup>-(3-chlorophenyl)-*N*<sup>2</sup>-(4-nitrophenyl)hydrazine-1,2-bis(carbothioamide)).
- Fig. S48.** FT-IR spectra of compound **3l** (*N*<sup>1</sup>-(3-chlorophenyl)-*N*<sup>2</sup>-(4-nitrophenyl)hydrazine-1,2-bis(carbothioamide)).
- Fig. S49.** Lineweaver-Burk plots of compound **3l** (*N*<sup>1</sup>-(3-chlorophenyl)-*N*<sup>2</sup>-(4-nitrophenyl)hydrazine-1,2-bis(carbothioamide)).

**Table S1.** FT-IR values of the novel asymmetric bis(carbothioamides) (**3a-l**) (cm<sup>-1</sup>).

Compounds ID	N <sup>1</sup> H	N <sup>2</sup> H	N <sup>3</sup> H	Ar H	Aliph. H	C=S	NO <sub>2</sub> <sup>a</sup>	C-N	Specific Peak	
<b>3a</b>	3265	3194	3119	3028	2949	1375	-	1189 1153 1097	-	
<b>3b</b>	3243	3195	3110	2999	2937	1338	-	1186 1169 1039	-	
<b>3c</b>	3206		3106	3004	2935	1337	-	1181 1102 1026	-	
<b>3d</b>		3181		3108	3010	2936	1336	-	1183 1160 1086	C-Cl: 958
<b>3e</b>	3212		3108		3007	2935	1334	-	1100 1070 1024	C-F: 1183
<b>3f</b>	3193		3105		3013	2936	1337	-	1184 1105 1069	-
<b>3g</b>	3393	3252	3155	3048	2914	1389	1505 1323	1186 1108 1046	-	
<b>3h</b>	3329	3205	3161	3082	2891	1352	1468 1321	1204 1109 1050	-	
<b>3i</b>	3218		3105		3006	2934	1295	1504 1344	1189 1103 1028	-
<b>3j</b>	3323	3214	3160	3043	2897	1323	1496 1297	1186 1002 961	C-F: 1107	
<b>3k</b>	3329	3272	3102	2991	2878	1372	1502 1330	1166 1104 1068	-	
<b>3l</b>	3327	3183	3072	3033	2812	1370	1476 1332	1241 1198 1110	C-Cl: 999	

<sup>a</sup> The asymmetric and symmetric stretching vibrations.

**Table S2.** ADME/T related parameters <sup>a</sup> of the novel asymmetric bis(carbothioamides) (**3a-l**) and clinically used reference inhibitor tacrine.

Compound ID	#stars	#rtVFG	CNS	MW	Dipole	SASA	Volume	donorHB	acctpHB	QPlogPC16	QPlogPoct	QPlogPw	QPlogS	QPPCaco	QPlogBB	QPPMDCK	QPlogKp	#metab	QPlogKhsa	HOA	PSA	Rule of Five	Rule of Three
<b>3a</b>	0	1	-1	254.37	2.0	535.2	859.9	4.0	5.0	9.7	4.0	5.0	4.0	1862	-0.9	4284	-1.9	1	-0.28	100	66.4	0	0
<b>3b</b>	0	1	-1	332.44	1.5	646.5	1065.0	4.0	5.8	12.9	4.0	5.8	4.0	1778	-0.2	4356	-1.3	3	0.34	100	73.3	0	0
<b>3c</b>	0	1	-1	332.44	1.5	647.6	1066.0	4.0	5.8	12.9	4.0	5.8	4.0	1830	-0.2	4784	-1.3	2	0.36	100	73.4	0	0
<b>3d</b>	1	1	0	336.86	2.3	637.7	1035.8	4.0	5.0	13.2	4.0	5.0	4.0	1780	0.0	10000	-1.4	1	0.10	100	65.1	0	1
<b>3e</b>	0	1	0	320.40	3.0	602.4	995.0	4.0	5.0	12.0	4.0	5.0	4.0	2228	0.5	8409	-1.2	2	0.22	100	64.8	0	0
<b>3f</b>	2	1	-1	316.44	2.4	646.3	1052.2	4.0	5.0	12.8	4.0	5.0	4.0	1778	-0.2	4573	-1.4	3	0.14	100	65.1	0	1
<b>3g</b>	1	1	-2	311.38	8.3	597.3	976.4	4.0	6.0	11.5	4.0	6.0	4.0	217	-1.3	418	-3.6	2	-0.23	80	111.2	0	0
<b>3h</b>	1	1	-2	377.44	6.8	686.4	1139.3	4.0	6.8	14.0	4.0	6.8	4.0	211	-1.4	435	-3.2	3	0.21	84	118.3	0	1
<b>3i</b>	1	1	-2	377.44	8.6	686.7	1139.6	4.0	6.8	14.0	4.0	6.8	4.0	217	-1.4	477	-3.2	2	0.22	85	118.4	0	1
<b>3j</b>	1	1	-2	365.40	6.6	661.1	1081.0	4.0	6.0	13.2	4.0	6.0	4.0	210	-1.2	821	-3.3	2	0.29	85	110.1	0	1
<b>3k</b>	1	1	-2	361.44	8.3	661.7	1108.7	4.0	6.0	13.8	4.0	6.0	4.0	246	-1.3	449	-3.0	2	0.67	86	110.8	0	0
<b>3l</b>	2	1	-2	381.85	6.7	676.2	1109.1	4.0	6.0	14.2	4.0	6.0	4.0	210	-1.2	1122	-3.3	2	0.93	87	110.1	0	1
<b>THA</b> <sup>b</sup>	0	0	1	198.27	4.2	430.7	709.9	1.5	2.0	6.9	10.7	6.4	-3.1	2931	0.0	1582	-1.8	3	0.71	100	34.2	0	0

<sup>a</sup> Various computational pharmacodynamic and pharmacokinetic parameters of synthesized compounds in this research were predicted such as number of property or descriptor values that fall outside the 95% range of similar values for known drugs. (#stars; 0 - 5), number of reactive functional groups (#rtVFG; 0 - 2), central nervous system activity (CNS; -2 inactive, +2 active), molecular weight of the compound (MW; 130.0 - 725.0), computed dipole moment of the compound (Dipole; 1.0 - 12.5), total solvent accessible surface area (SASA; 300.0 - 1000.0), total solvent-accessible volume in cubic angstroms using a probe with a 1.4 Å Radius (Volume; 500.0 - 2000.0), number of hydrogen bonds that would be donated by the solute to water molecules in an aqueous solution (donorHB; 0.0 - 6.0), number of hydrogen bonds that would be accepted by the solute from water molecules in an aqueous solution (acctpHB; 2.0 - 20.0), hexadecane/gas partition coefficient (QPlogPC16; 4.0 - 18.0), octanol/gas partition coefficient (QPlogPoct; 8.0 - 35.0), water/gas partition coefficient (QPlogPw; 4.0 - 45.0), aqueous solubility (QPlogS; -6.5 - 0.5), apparent Caco-2 cell permeability in nm/sec (QPPCaco; <25 poor, great>500), brain/blood partition coefficient (QPlogBB; -3.0 - 1.2), apparent MDCK cell permeability in nm/sec (QPPMDCK; <25 poor, great>500), skin permeability (QPlogKp; -8.0 - -1.0), number of likely metabolic reactions (#metab; 1 - 8), prediction of binding to human serum albumin (QPlogKhsa; -1.5 - 1.5), human oral absorption (HOA; <25% poor, high>80%), van der Waals surface area of polar nitrogen and oxygen atoms (PSA; 7.0 - 200.0), number of violations of Lipinski's rule of five (max. 4), and number of violations of Jorgensen's rule of three (max. 3).

<sup>b</sup> Tacrine.

**Table S3.** Pharmacokinetic properties <sup>a</sup> of the novel asymmetric bis(carbothioamides) (**3a-l**) and clinically used reference inhibitor tacrine.

Compounds ID	GI absorption	BBB permeant	P-gp substrate	CYP inhibitor				
				CYP1A2	CYP2C19	CYP2C9	CYP2D6	CYP3A4
<b>3a</b>	High	No	No	No	Yes	No	No	No
<b>3b</b>	High	No	No	No	Yes	Yes	Yes	No
<b>3c</b>	High	No	No	No	Yes	Yes	Yes	No
<b>3d</b>	High	No	No	No	Yes	Yes	No	Yes
<b>3e</b>	High	No	No	No	Yes	Yes	No	Yes
<b>3f</b>	High	No	No	No	Yes	Yes	No	Yes
<b>3g</b>	Low	No	No	No	No	No	No	No
<b>3h</b>	Low	No	No	No	No	Yes	Yes	No
<b>3i</b>	Low	No	No	No	No	Yes	Yes	No
<b>3j</b>	Low	No	No	No	No	Yes	No	No
<b>3k</b>	Low	No	No	No	No	Yes	No	No
<b>3l</b>	Low	No	No	No	No	Yes	No	No
<b>THA</b> <sup>b</sup>	High	Yes	Yes	Yes	No	No	No	Yes

<sup>a</sup> Various pharmacokinetic parameters, such as the GI absorption, human gastrointestinal absorption; BBB permeant, blood-brain barrier permeation; P-gp substrate, prediction of being substrate or non-substrate of P-glycoprotein; CYP inhibitor, prediction of being inhibitor or non-inhibitor of cytochromes P450 (CYP) five major isoforms (CYP1A2, CYP2C19, CYP2C9, CYP2D6, CYP3A4); and log  $K_p$ , prediction of the skin permeability coefficient of targeted compounds in this research, were predicted using SwissADME platform.

<sup>b</sup> Tacrine.

**Table S4.** Drug-likeness descriptors <sup>a</sup> of the novel asymmetric bis(carbothioamides) (**3a-l**) and clinically used reference inhibitor tacrine.

Compounds ID	Ghose	Veber	Egan	Muegge	Bioavailability Score
<b>3a</b>	Yes	Yes	Yes	Yes	0.55
<b>3b</b>	Yes	Yes	Yes	Yes	0.55
<b>3c</b>	Yes	Yes	Yes	Yes	0.55
<b>3d</b>	Yes	Yes	Yes	Yes	0.55
<b>3e</b>	Yes	Yes	Yes	Yes	0.55
<b>3f</b>	Yes	Yes	Yes	Yes	0.55
<b>3g</b>	Yes	No; 1 violation: TPSA>140	No; 1 violation: TPSA>131.6	No; 1 violation: TPSA>150	0.55
<b>3h</b>	Yes	No; 1 violation: TPSA>140	No; 1 violation: TPSA>131.6	No; 1 violation: TPSA>150	0.55
<b>3i</b>	Yes	No; 1 violation: TPSA>140	No; 1 violation: TPSA>131.6	No; 1 violation: TPSA>150	0.55
<b>3j</b>	Yes	No; 1 violation: TPSA>140	No; 1 violation: TPSA>131.6	No; 1 violation: TPSA>150	0.55
<b>3k</b>	Yes	No; 1 violation: TPSA>140	No; 1 violation: TPSA>131.6	No; 1 violation: TPSA>150	0.55
<b>3l</b>	Yes	No; 1 violation: TPSA>140	No; 1 violation: TPSA>131.6	No; 1 violation: TPSA>150	0.55
<b>THA</b> <sup>b</sup>	Yes	Yes	Yes	No; 1 violation: MW<200	0.55

<sup>a</sup> Drug-likeness parameters, such as the Ghose (Amgen), Veber (GSK), Egan (Pharmacia), and Muegge (Bayer) methods and bioavailability score (Abbot) of targeted compounds in this research, were predicted using SwissADME platform.

<sup>b</sup> Tacrine.



**Table S5.** Medicinal Chemistry pattern recognition methods <sup>a</sup> of the novel asymmetric bis(carbothioamides) (**3a-l**) and clinically used reference inhibitor tacrine.

Compounds ID	PAINS	Brenk	Lead-likeness	SA score
<b>3a</b>	0 alert	1 alert: thiocarbonyl group	Yes	2.52
<b>3b</b>	0 alert	1 alert: thiocarbonyl group	No; 1 violation: Rotors>7	2.78
<b>3c</b>	0 alert	1 alert: thiocarbonyl group	No; 1 violation: Rotors>7	2.61
<b>3d</b>	0 alert	1 alert: thiocarbonyl group	No; 1 violation: XLOGP3>3.5	2.67
<b>3e</b>	0 alert	1 alert: thiocarbonyl group	Yes	2.88
<b>3f</b>	0 alert	1 alert: thiocarbonyl group	Yes	2.54
<b>3g</b>	0 alert	4 alerts: isolated alkene, nitro group, oxygen-nitrogen single bond, thiocarbonyl group	No; 1 violation: Rotors>7	2.82
<b>3h</b>	0 alert	3 alerts: nitro group, oxygen-nitrogen single bond, thiocarbonyl group	No; 2 violations: MW>350, Rotors>7	2.99
<b>3i</b>	0 alert	3 alerts: nitro group, oxygen-nitrogen single bond, thiocarbonyl group	No; 2 violations: MW>350, Rotors>7	2.86
<b>3j</b>	0 alert	3 alerts: nitro group, oxygen-nitrogen single bond, thiocarbonyl group	No; 2 violations: MW>350, Rotors>7	2.91
<b>3k</b>	0 alert	3 alerts: nitro group, oxygen-nitrogen single bond, thiocarbonyl group	No; 2 violations: MW>350, Rotors>7	2.79
<b>3l</b>	0 alert	3 alerts: nitro group, oxygen-nitrogen single bond, thiocarbonyl group	No; 2 violations: MW>350, Rotors>7	2.90
<b>THA <sup>b</sup></b>	0 alert	0 alert	No; 1 violation: MW>350	2.08

<sup>a</sup> Medicinal Chemistry pattern recognition method, such as the PAINS, pan assay interference structure alert filter; Brenk, structural alert filter; Lead-likeness, lead-likeness criteria; and SA score, synthetic accessibility score (ranges from 1, very easy, to 10, very difficult) of targeted compounds in this research, were predicted using SwissADME platform.

<sup>b</sup> Tacrine.

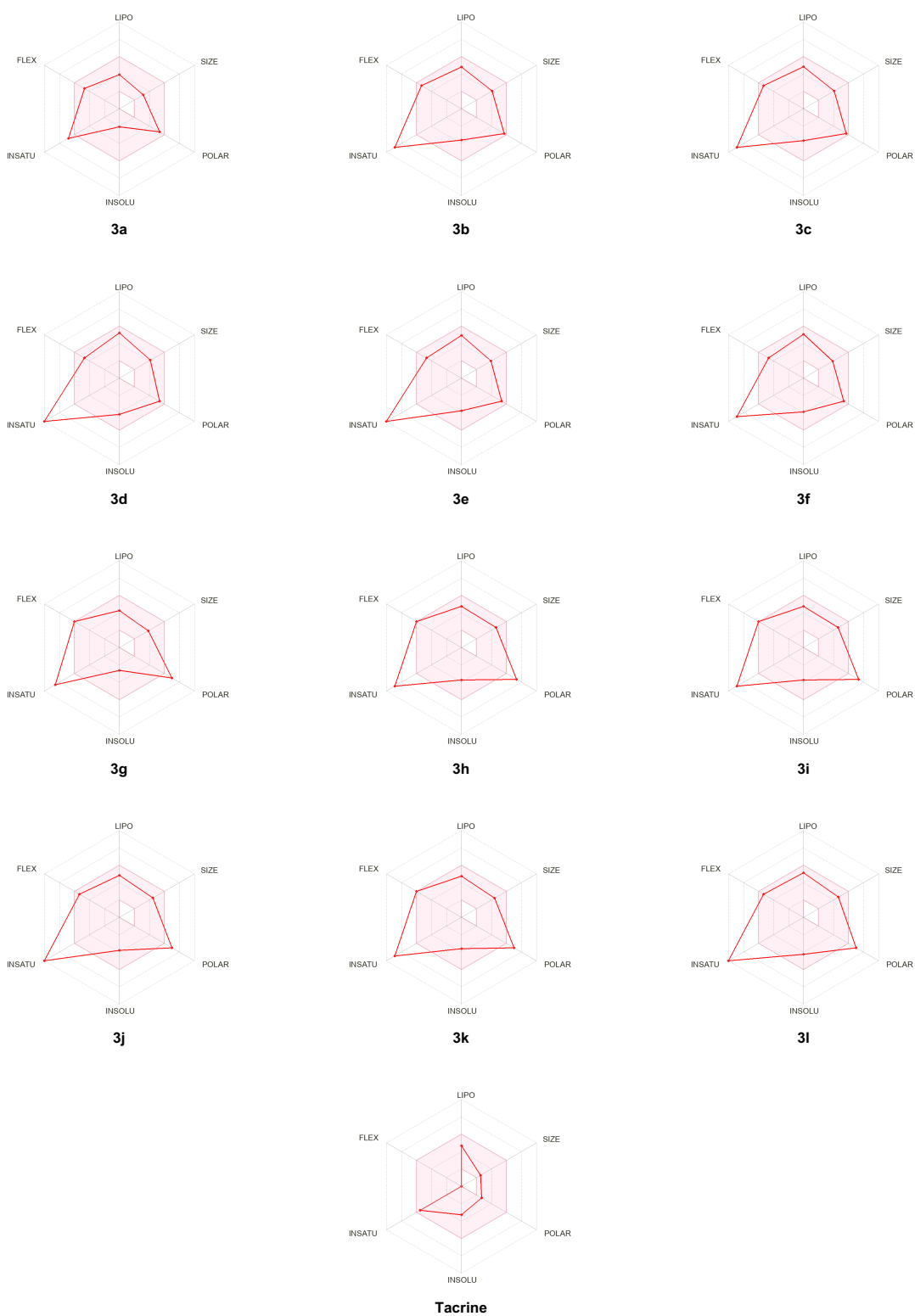


**Fig. S1.** Diagrams showing 'drug-likeness' descriptors for the novel asymmetric bis(carbothioamides) (3a-l) and clinically used reference inhibitor tacrine. The red-colored zone has been identified as a feasible physicochemical domain to enhance oral bioavailability. LIPO, lipophilicity; SIZE, molecular weight; POLAR, polarity; INSOLU, insolubility; INSATU, saturation; and FLEX, flexibility.

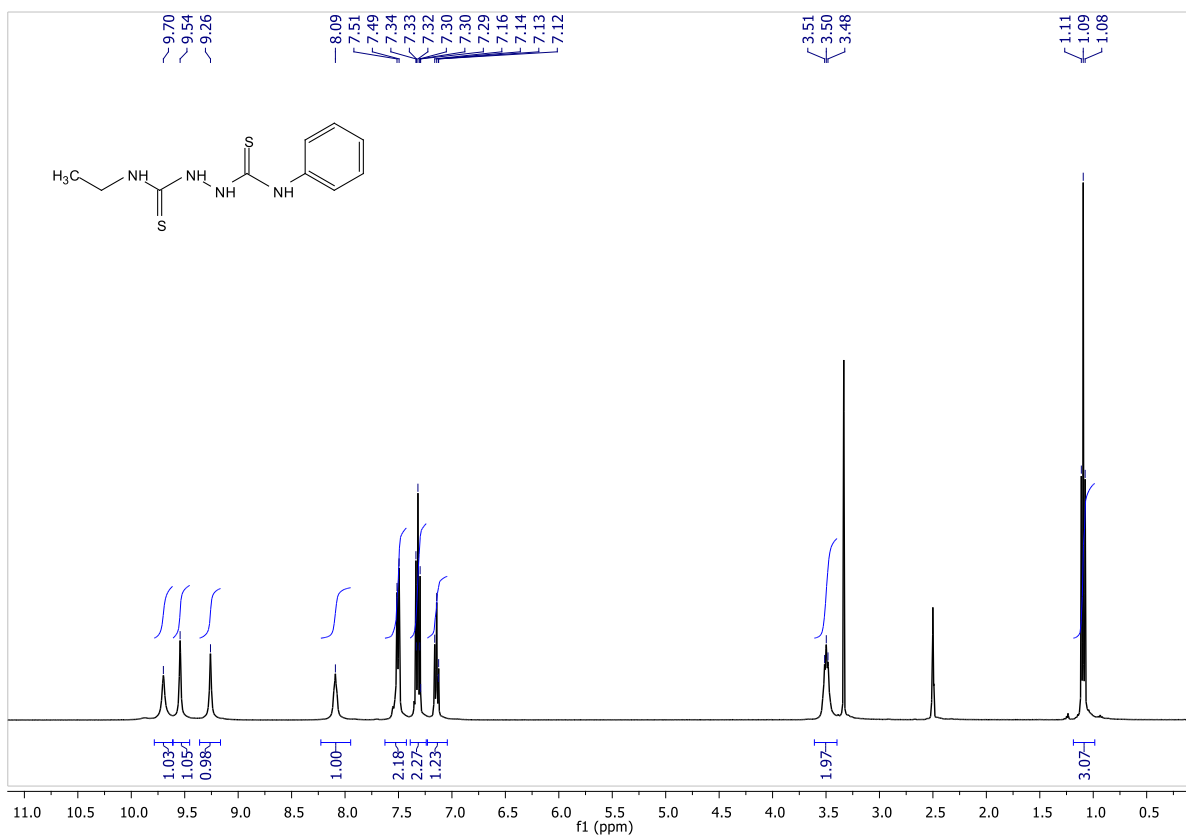


**Fig. S2.**  $^1\text{H}$ -NMR (400 MHz,  $\text{DMSO-d}_6$ ) spectra of compound **3a** ( $N^1$ -ethyl- $N^2$ -phenylhydrazine-1,2-bis(carbothioamide)).

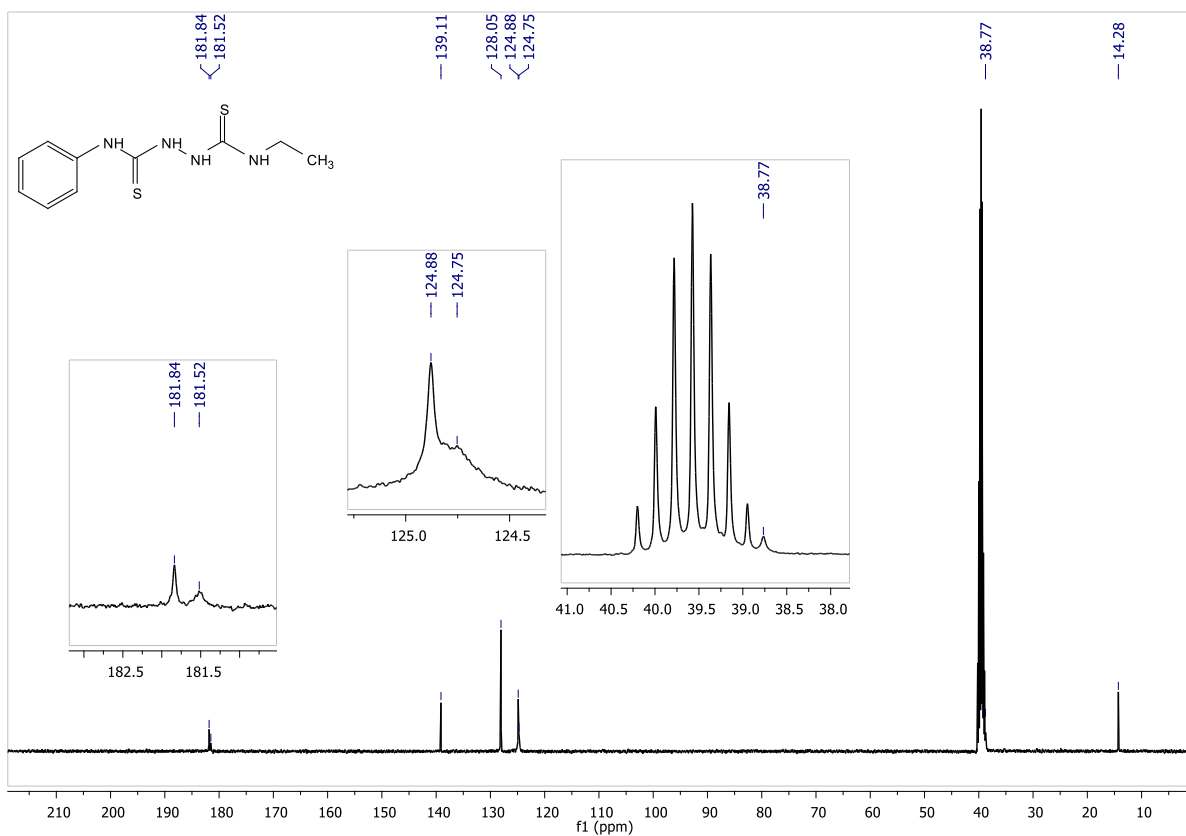


**Fig. S3.** <sup>13</sup>C-NMR (100 MHz, DMSO-*d*<sub>6</sub>) spectra of compound **3a** (*N*<sup>1</sup>-ethyl-*N*<sup>2</sup>-phenylhydrazine-1,2-bis(carbothioamide)).

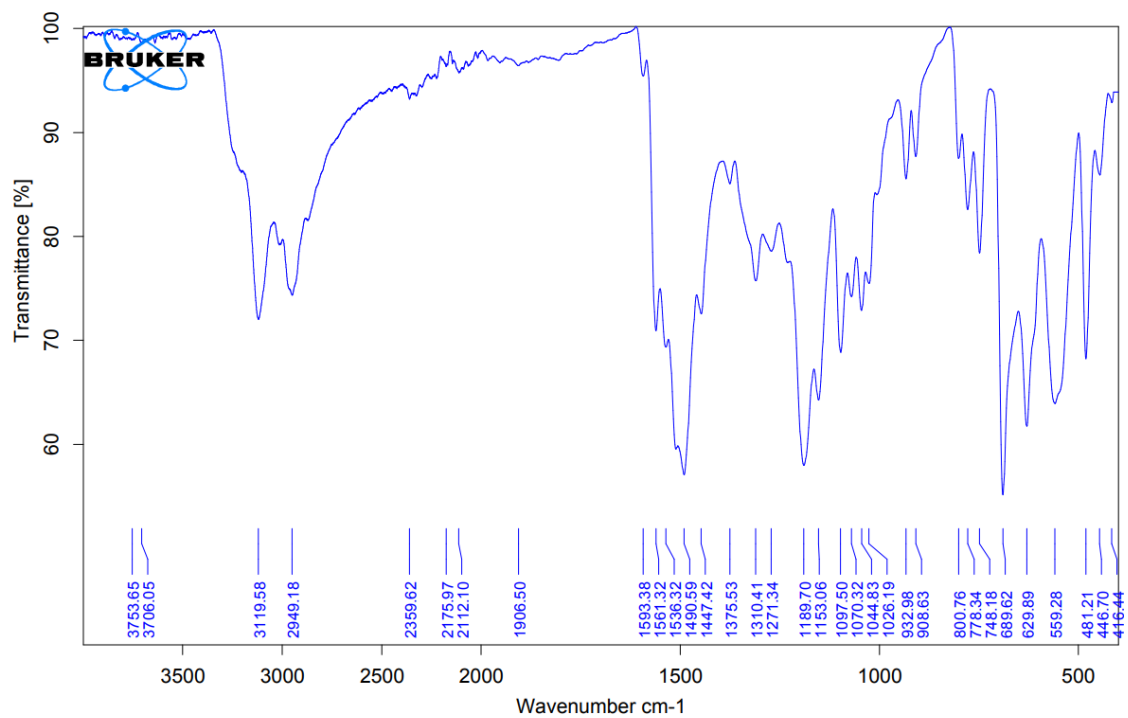


**Fig. S4.** FT-IR spectra of compound **3a** (*N*<sup>1</sup>-ethyl-*N*<sup>2</sup>-phenylhydrazine-1,2-bis(carbothioamide)).

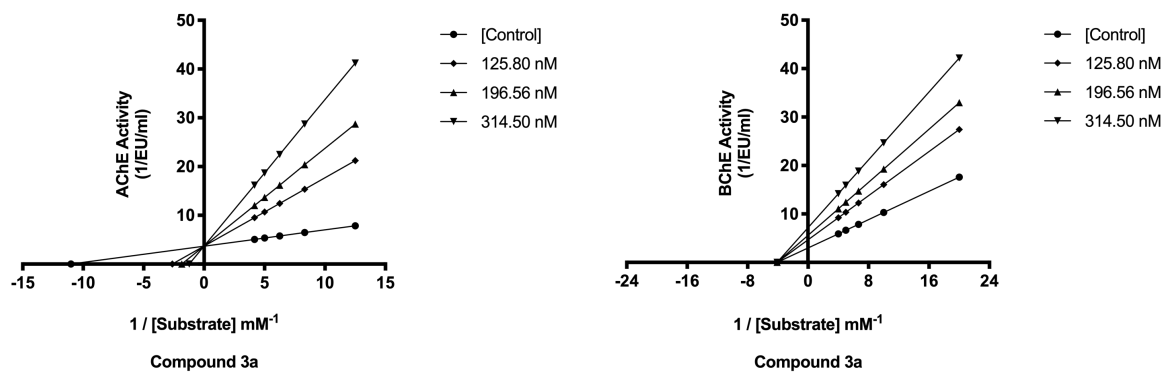


**Fig. S5.** Lineweaver-Burk plots of compound **3a** (*N*<sup>1</sup>-ethyl-*N*<sup>2</sup>-phenylhydrazine-1,2-bis(carbothioamide)).

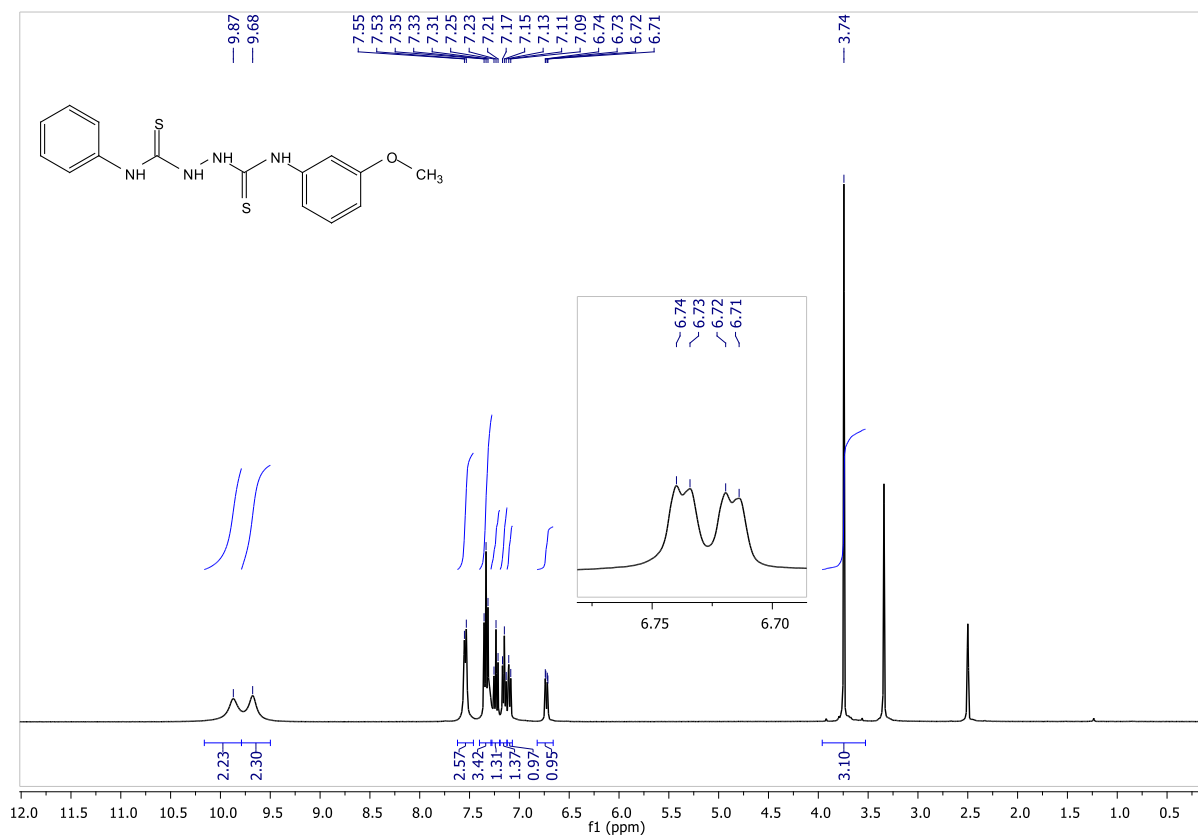


**Fig. S6.**  $^1\text{H-NMR}$  (400 MHz,  $\text{DMSO-}d_6$ ) spectra of compound **3b** ( $N^1$ -(3-methoxyphenyl)- $N^2$ -phenylhydrazine-1,2-bis(carbothioamide)).

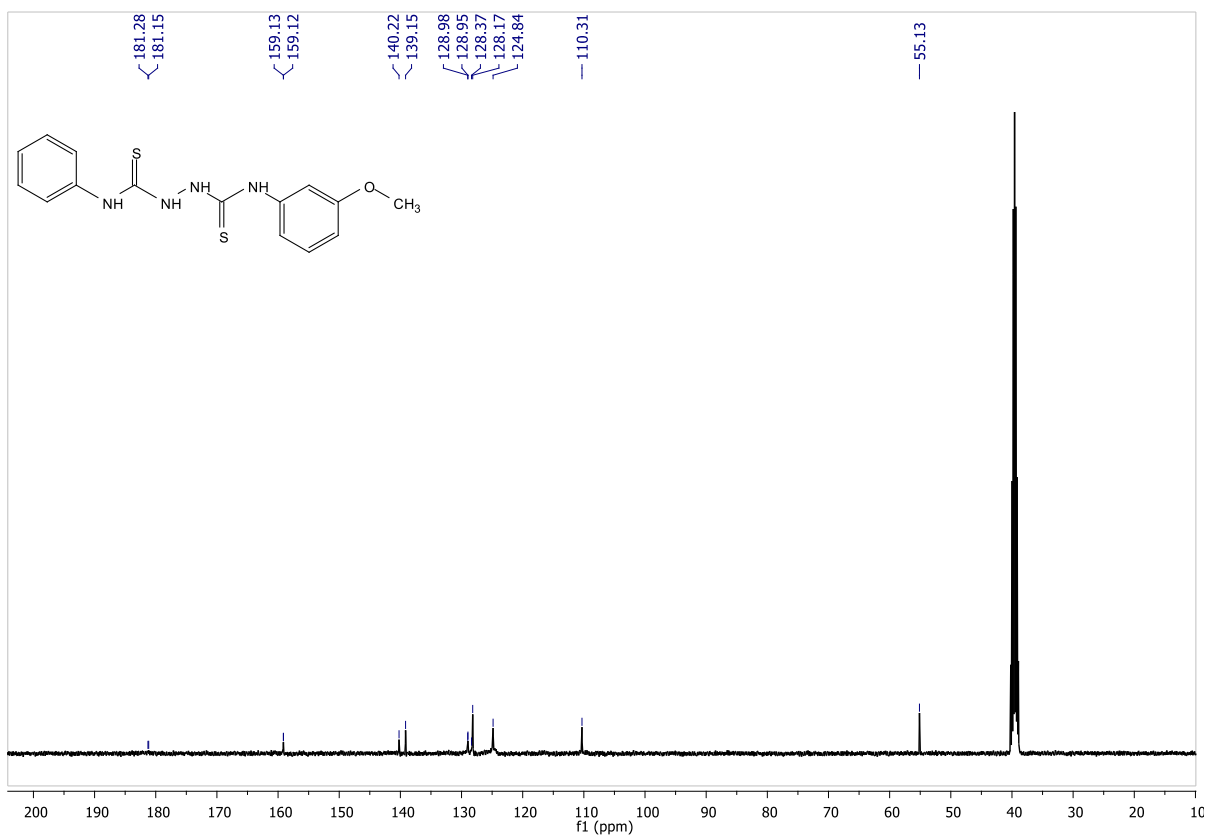


**Fig. S7.** <sup>13</sup>C-NMR (100 MHz, DMSO-*d*<sub>6</sub>) spectra of compound **3b** (*N*<sup>1</sup>-(3-methoxyphenyl)-*N*<sup>2</sup>-phenylhydrazine-1,2-bis(carbothioamide)).



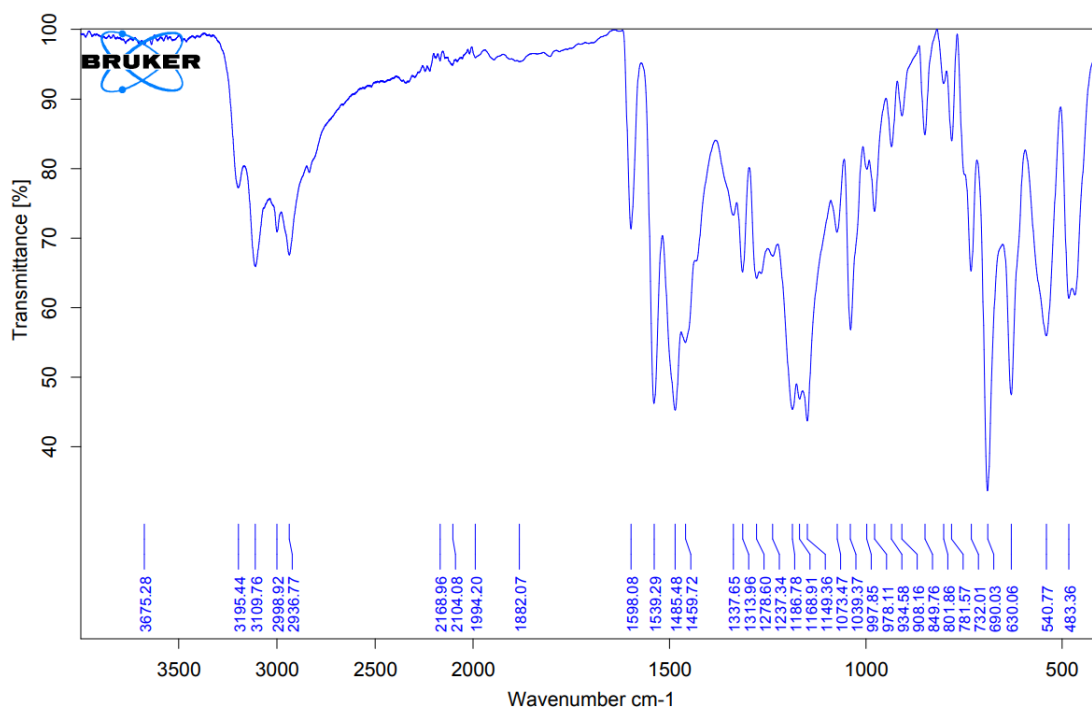


**Fig. S8.** FT-IR spectra of compound **3b** (*N*<sup>1</sup>-(3-methoxyphenyl)-*N*<sup>2</sup>-phenylhydrazine-1,2-bis(carbothioamide)).

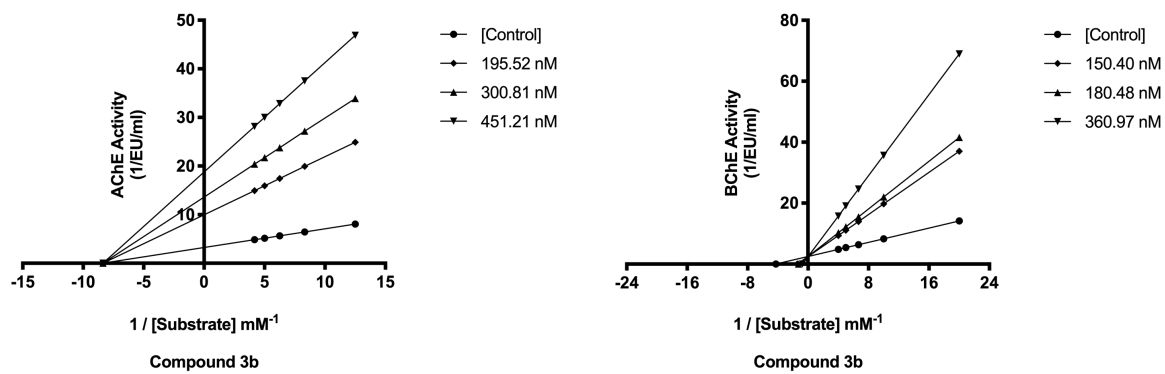


**Fig. S9.** Lineweaver-Burk plots of compound **3b** (*N*<sup>1</sup>-(3-methoxyphenyl)-*N*<sup>2</sup>-phenylhydrazine-1,2-bis(carbothioamide)).

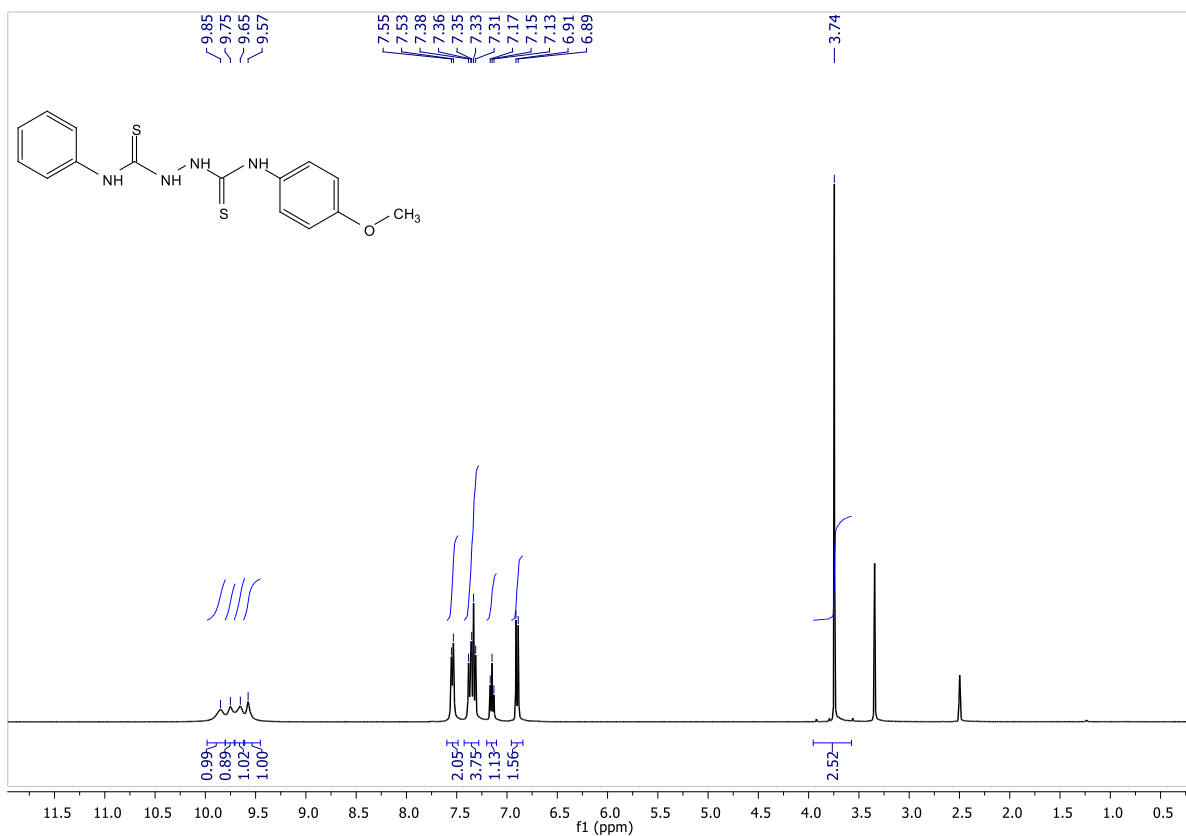


**Fig. S10.** <sup>1</sup>H-NMR (400 MHz, DMSO-*d*<sub>6</sub>) spectra of compound **3c** (*N*<sup>1</sup>-(4-methoxyphenyl)-*N*<sup>2</sup>-phenylhydrazine-1,2-bis(carbothioamide)).

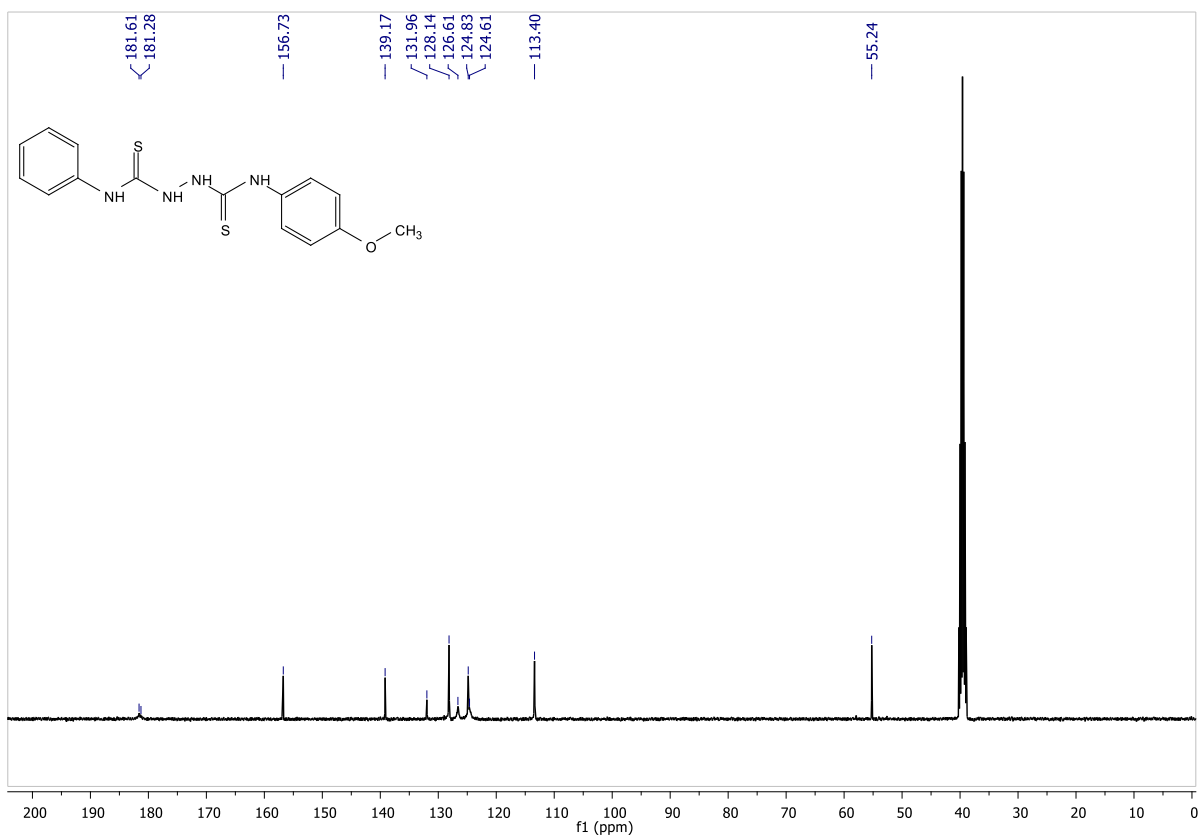


**Fig. S11.** <sup>13</sup>C-NMR (100 MHz, DMSO-*d*<sub>6</sub>) spectra of compound **3c** (*N*<sup>1</sup>-(4-methoxyphenyl)-*N*<sup>2</sup>-phenylhydrazine-1,2-bis(carbothioamide)).

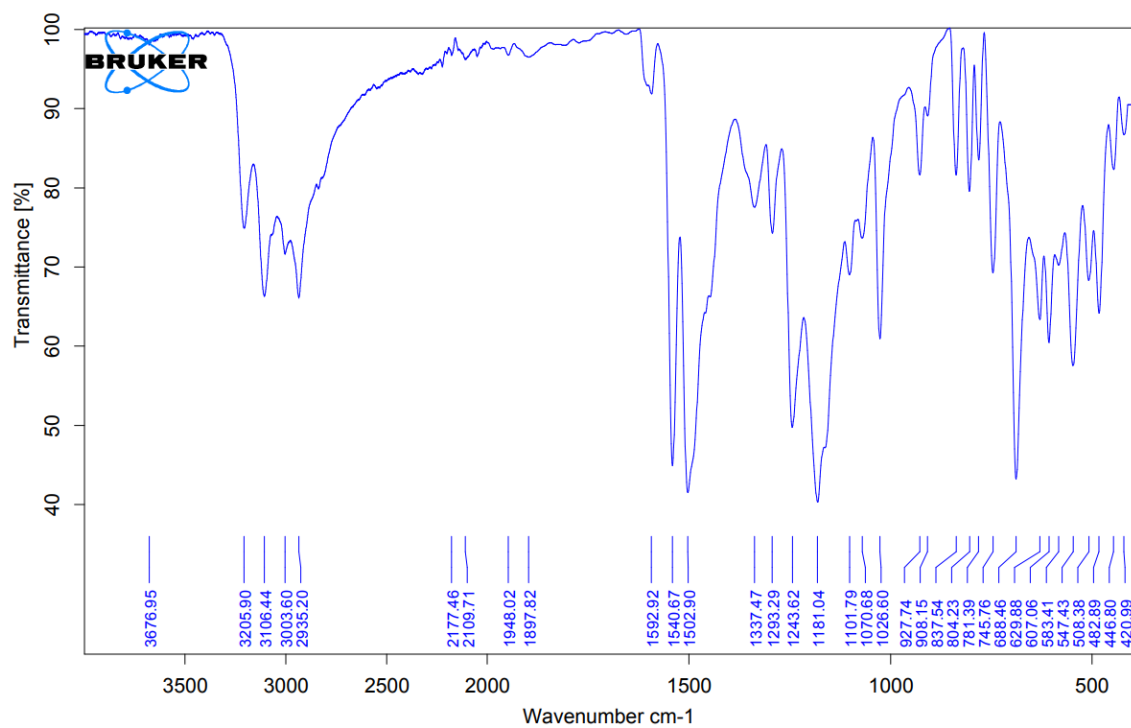


**Fig. S12.** FT-IR spectra of compound **3c** (*N*<sup>1</sup>-(4-methoxyphenyl)-*N*<sup>2</sup>-phenylhydrazine-1,2-bis(carbothioamide)).

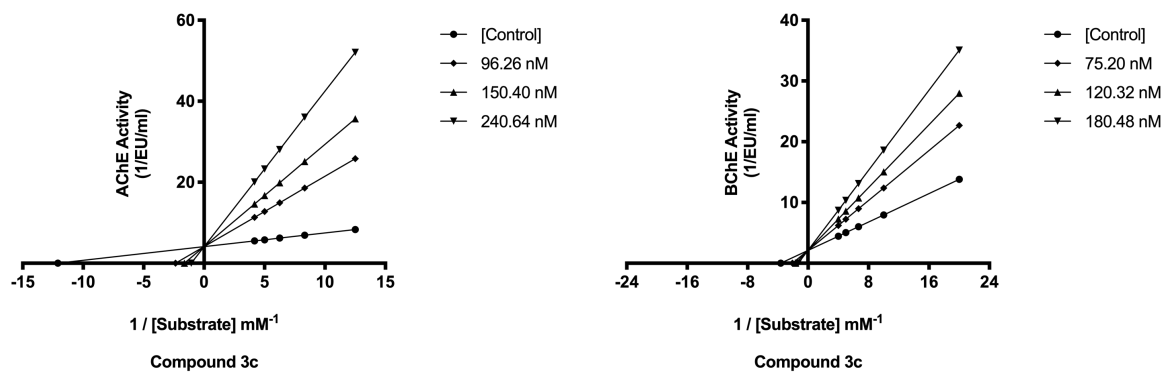


**Fig. S13.** Lineweaver-Burk plots of compound **3c** (*N*<sup>1</sup>-(4-methoxyphenyl)-*N*<sup>2</sup>-phenylhydrazine-1,2-bis(carbothioamide)).

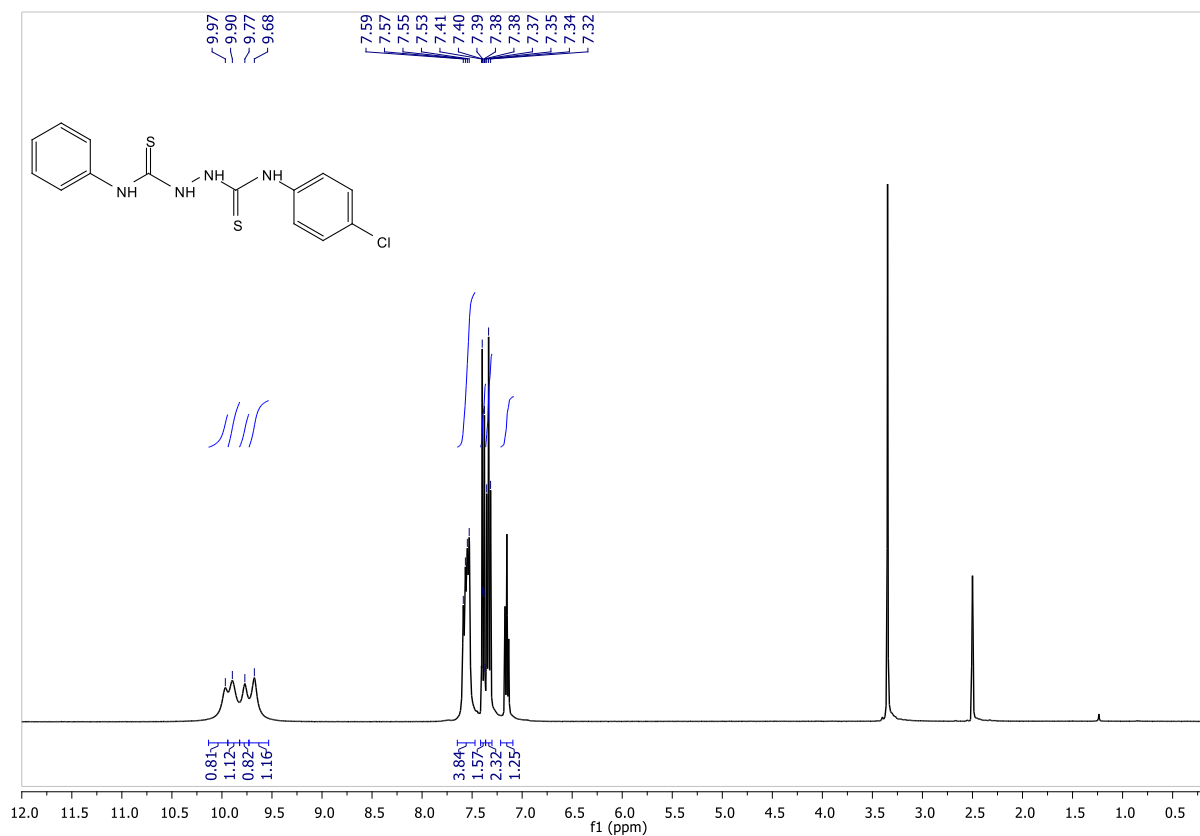


**Fig. S14.**  $^1\text{H-NMR}$  (400 MHz,  $\text{DMSO-}d_6$ ) spectra of compound **3d** ( $N^1$ -(4-chlorophenyl)- $N^2$ -phenylhydrazine-1,2-bis(carbothioamide)).

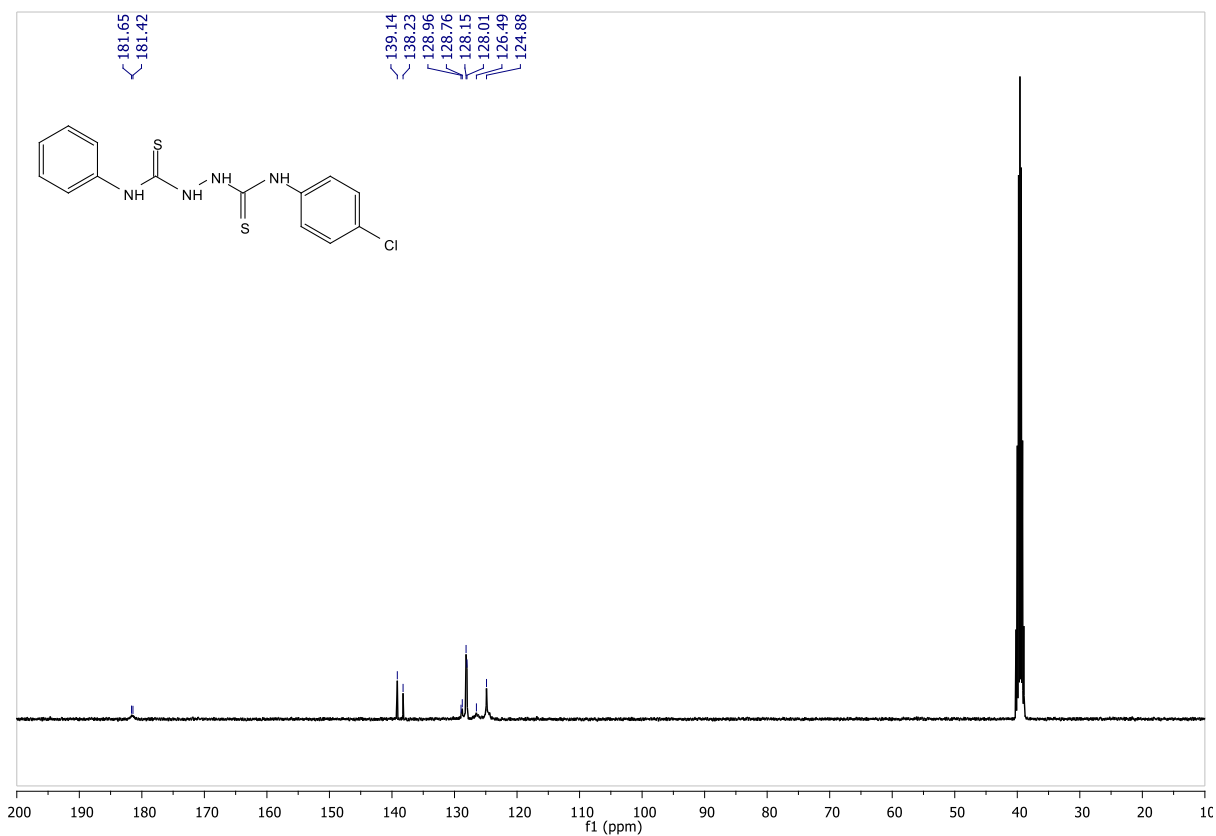


**Fig. S15.** <sup>13</sup>C-NMR (100 MHz, DMSO-*d*<sub>6</sub>) spectra of compound **3d** (*N*<sup>1</sup>-(4-chlorophenyl)-*N*<sup>2</sup>-phenylhydrazine-1,2-bis(carbothioamide)).



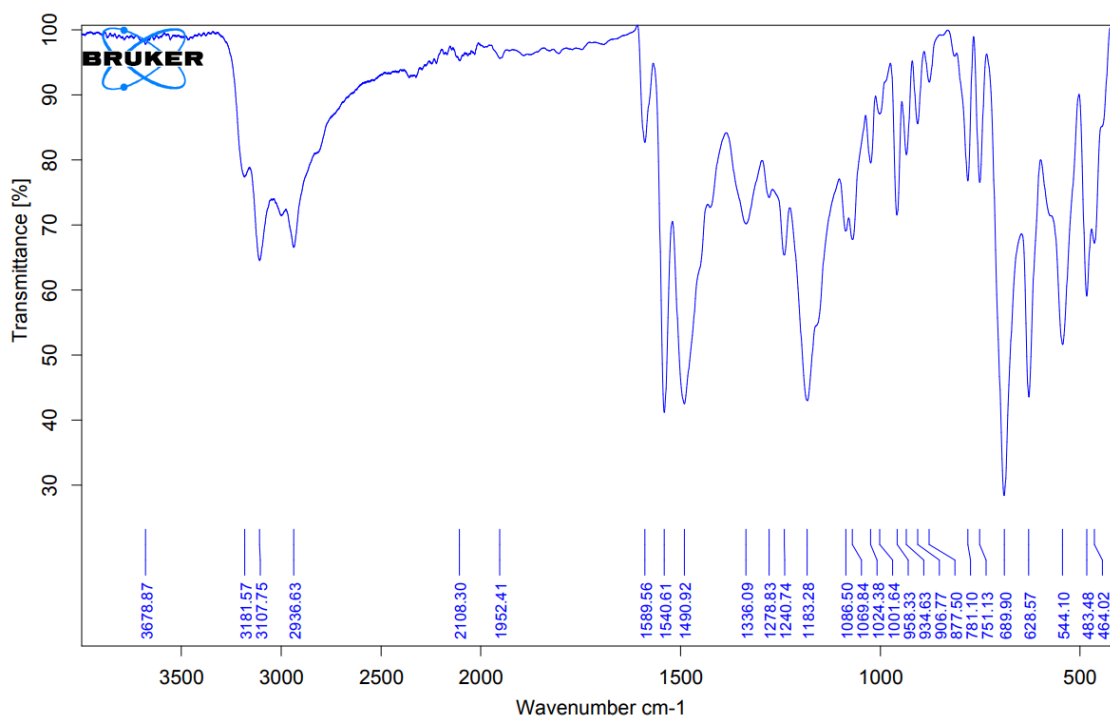


**Fig. S16.** FT-IR spectra of compound **3d** (*N*<sup>1</sup>-(4-chlorophenyl)-*N*<sup>2</sup>-phenylhydrazine-1,2-bis(carbothioamide)).

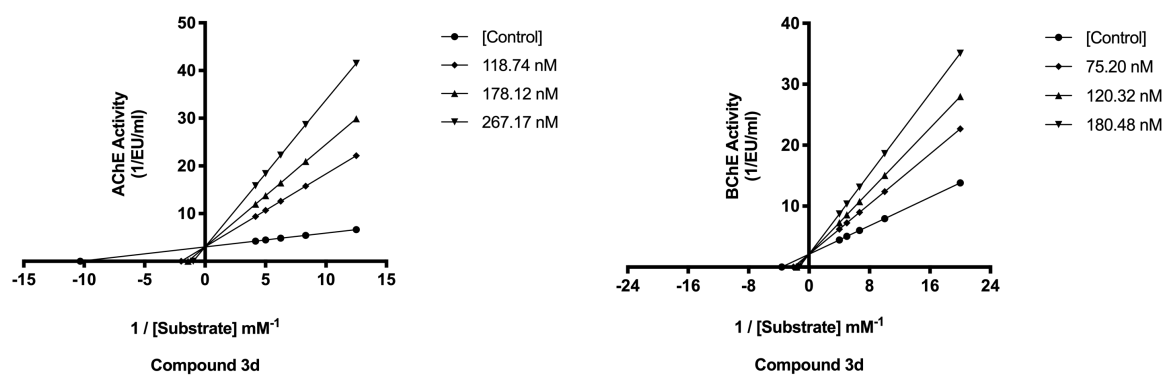


**Fig. S17.** Lineweaver-Burk plots of compound **3d** (*N*<sup>1</sup>-(4-chlorophenyl)-*N*<sup>2</sup>-phenylhydrazine-1,2-bis(carbothioamide)).

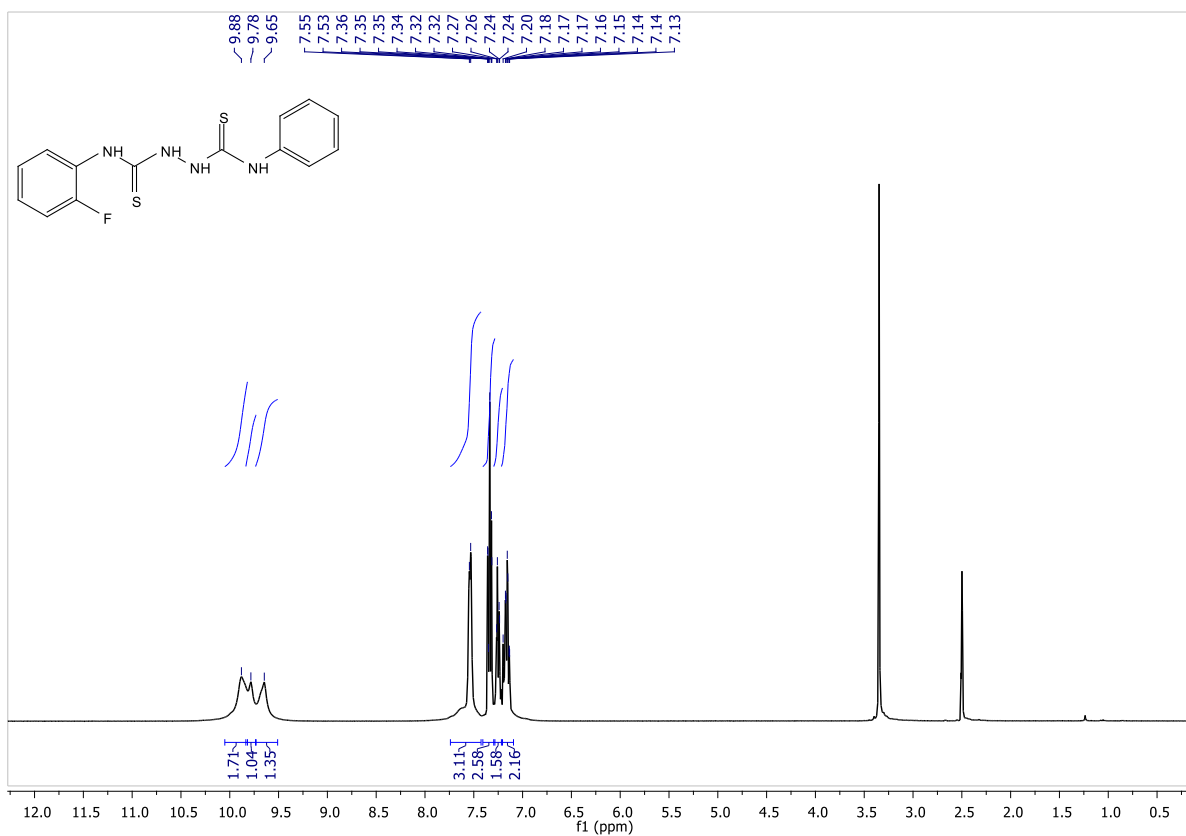


**Fig. S18.** <sup>1</sup>H-NMR (400 MHz, DMSO-*d*<sub>6</sub>) spectra of compound **3e** (*N*<sup>1</sup>-(2-fluorophenyl)-*N*<sup>2</sup>-phenylhydrazine-1,2-bis(carbothioamide)).

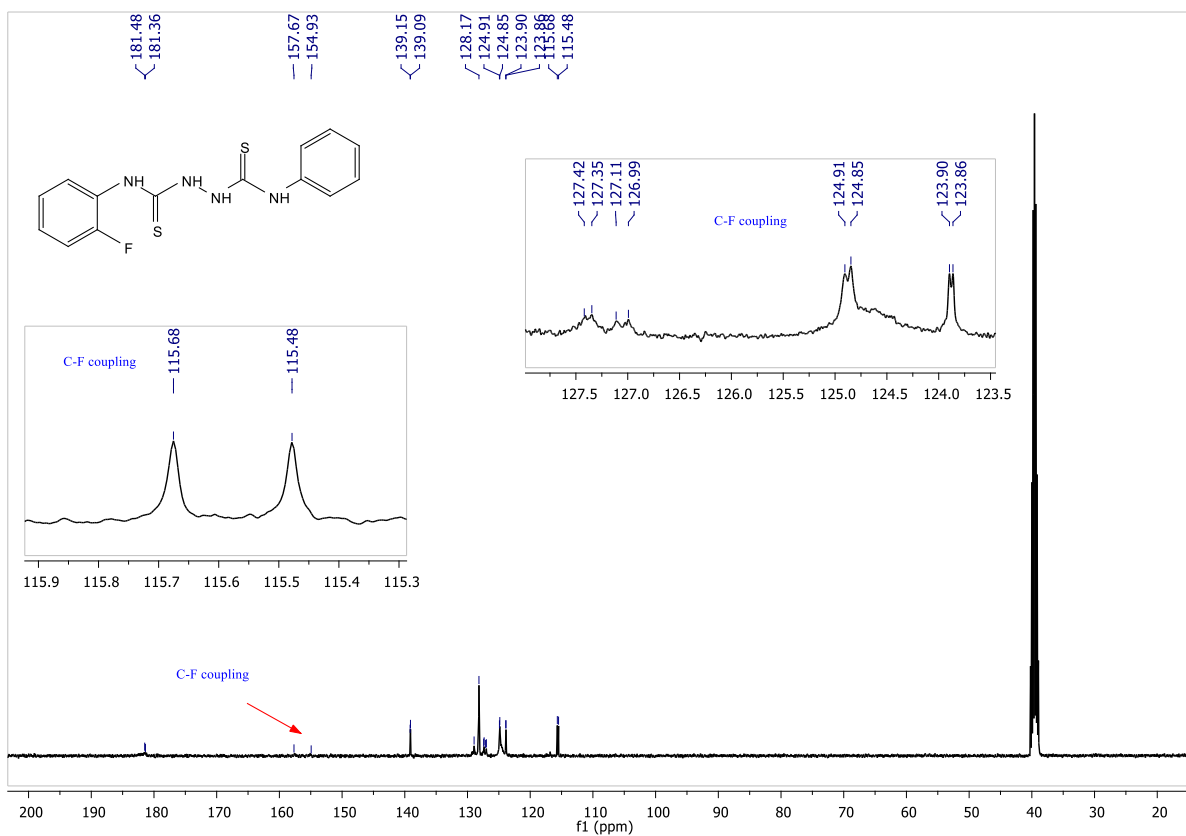


**Fig. S19.**  $^{13}\text{C}$ -NMR (100 MHz,  $\text{DMSO-}d_6$ ) spectra of compound **3e** ( $N^1$ -(2-fluorophenyl)- $N^2$ -phenylhydrazine-1,2-bis(carbothioamide)).

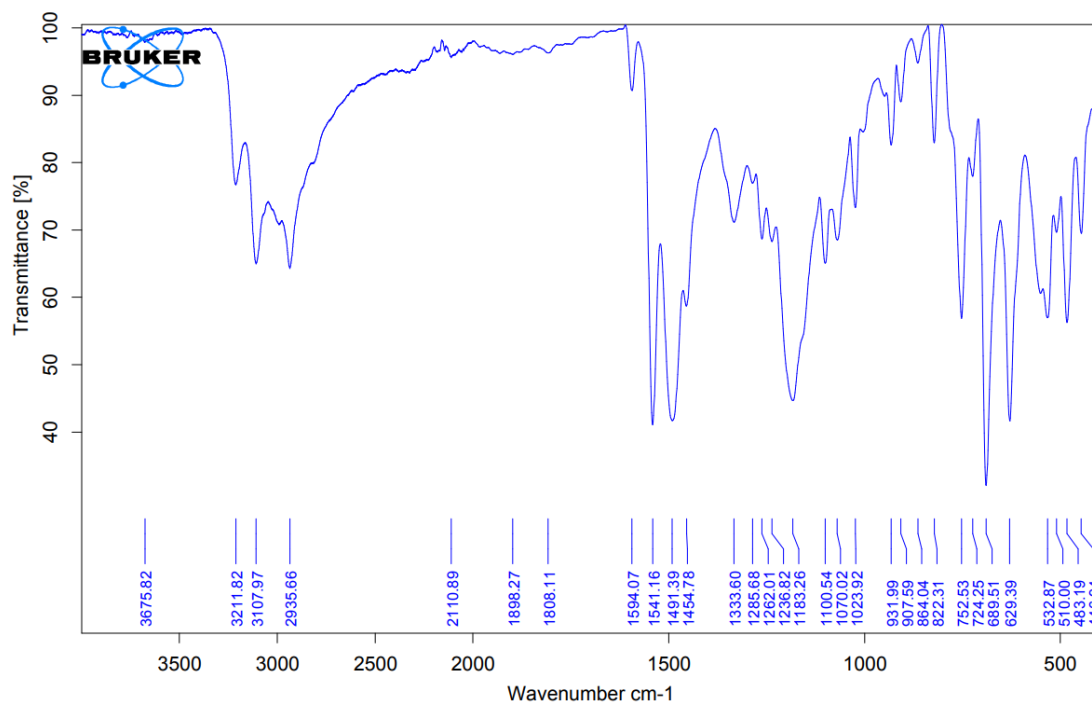


**Fig. S20.** FT-IR spectra of compound **3e** (*N*<sup>1</sup>-(2-fluorophenyl)-*N*<sup>2</sup>-phenylhydrazine-1,2-bis(carbothioamide)).

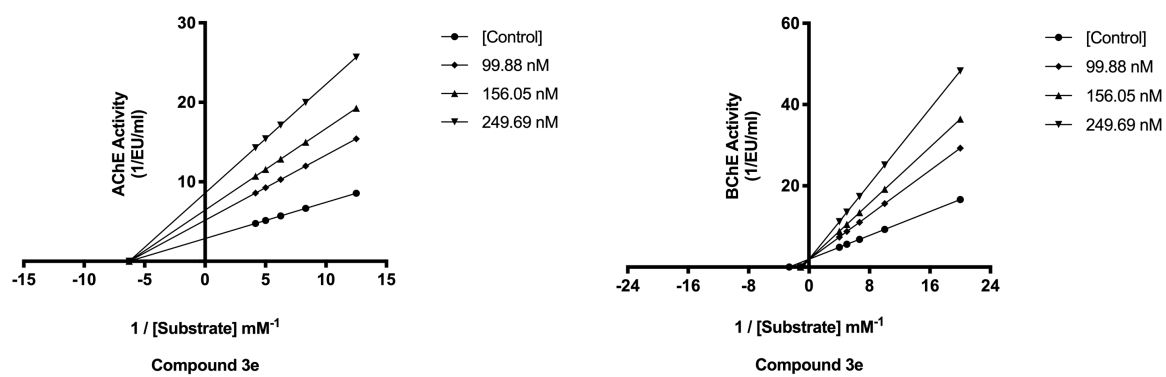


**Fig. S21.** Lineweaver-Burk plots of compound **3e** ( $N^1$ -(2-fluorophenyl)- $N^2$ -phenylhydrazine-1,2-bis(carbothioamide)).

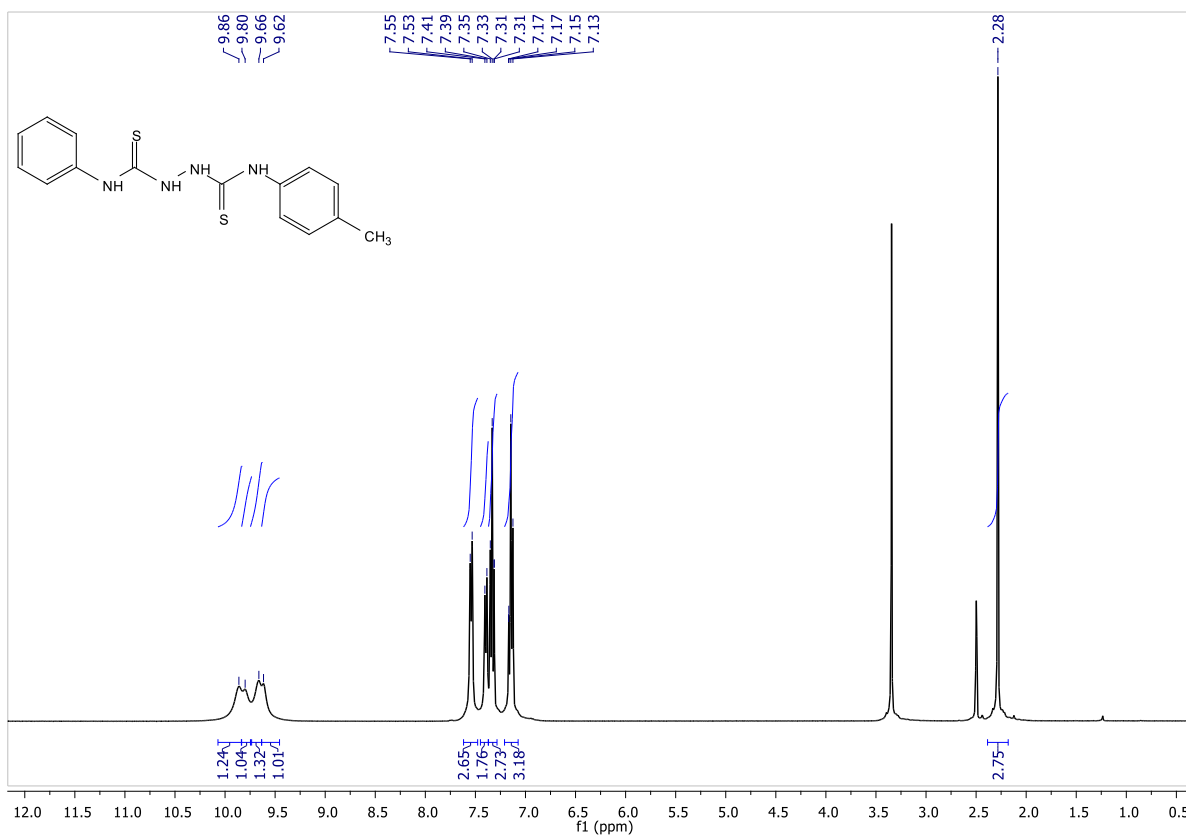


**Fig. S22.**  $^1\text{H-NMR}$  (400 MHz,  $\text{DMSO-}d_6$ ) spectra of compound **3f** ( $N^1$ -phenyl- $N^2$ -(*p*-tolyl)hydrazine-1,2-bis(carbothioamide)).

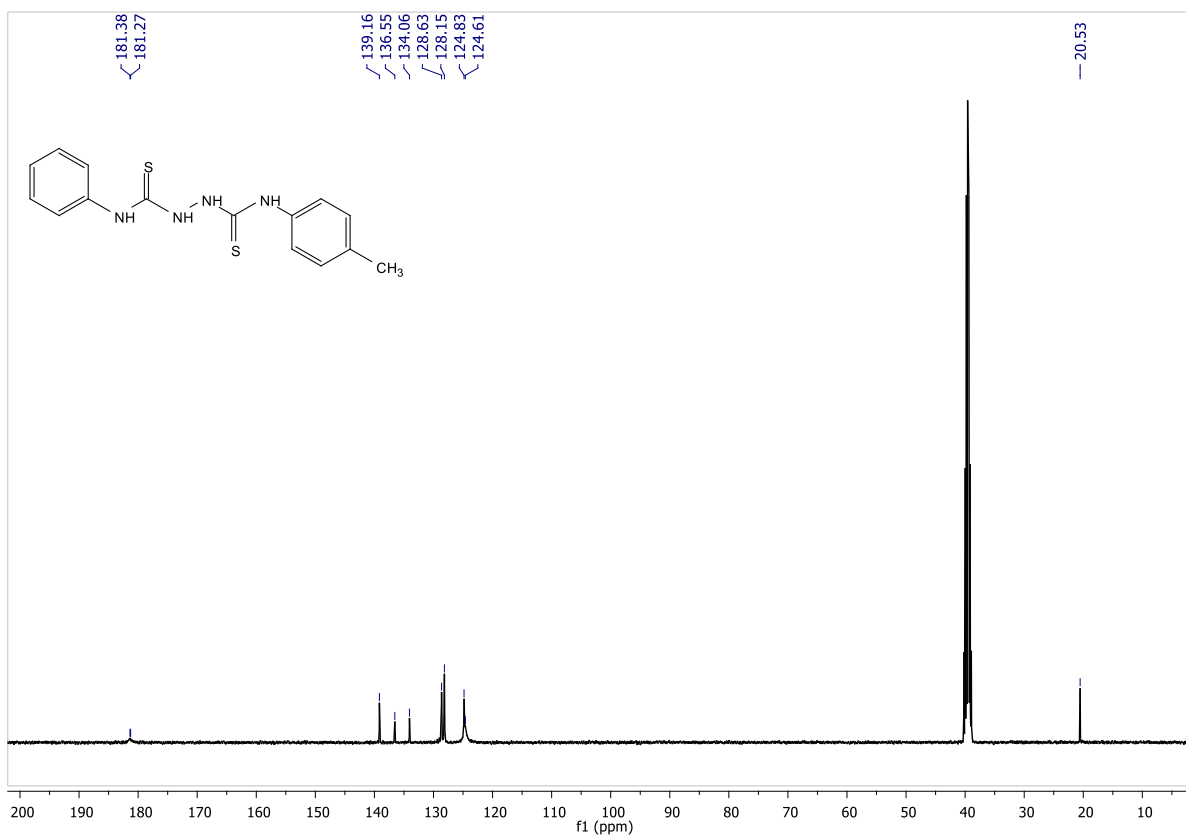


**Fig. S23.** <sup>13</sup>C-NMR (100 MHz, DMSO-*d*<sub>6</sub>) spectra of compound **3f** (*N*<sup>1</sup>-phenyl-*N*<sup>2</sup>-(*p*-tolyl)hydrazine-1,2-bis(carbothioamide)).



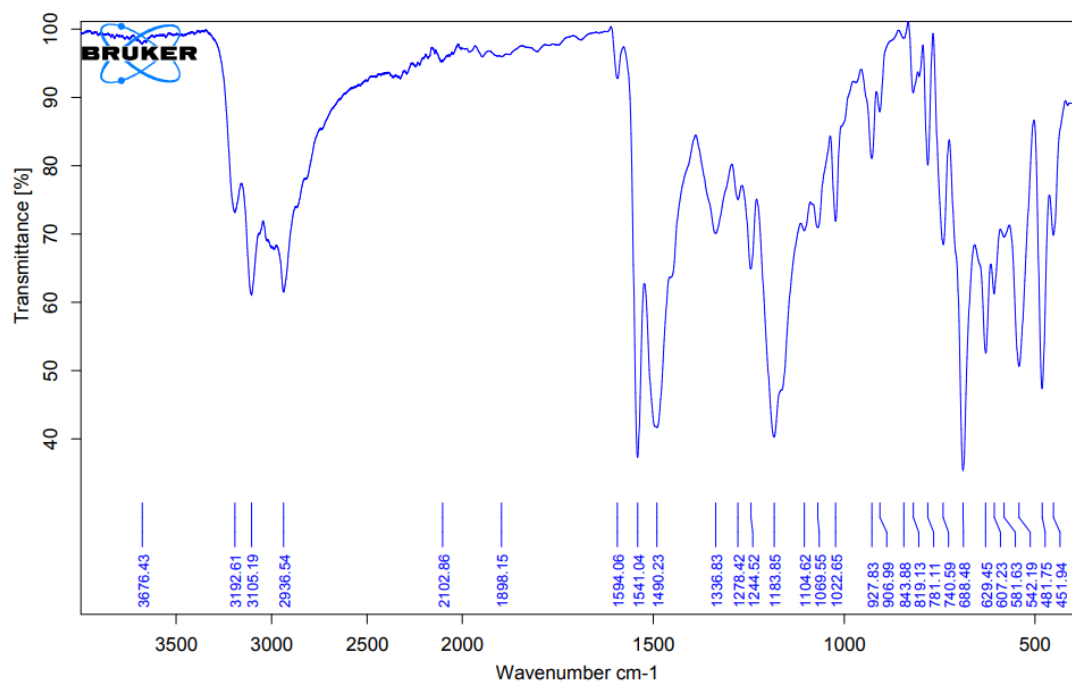


**Fig. S24.** FT-IR spectra of compound **3f** (*N*<sup>1</sup>-phenyl-*N*<sup>2</sup>-(*p*-tolyl)hydrazine-1,2-bis(carbothioamide)).

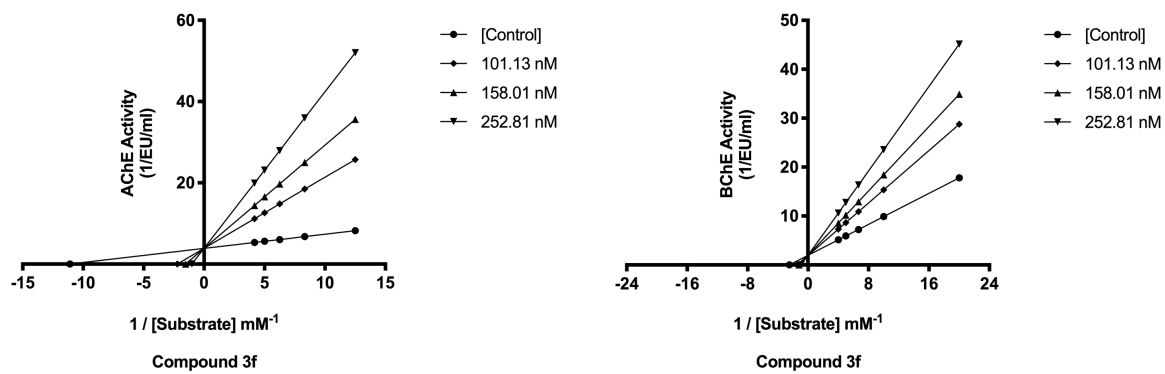


**Fig. S25.** Lineweaver-Burk plots of compound **3f** (*N*<sup>1</sup>-phenyl-*N*<sup>2</sup>-(*p*-tolyl)hydrazine-1,2-bis(carbothioamide)).

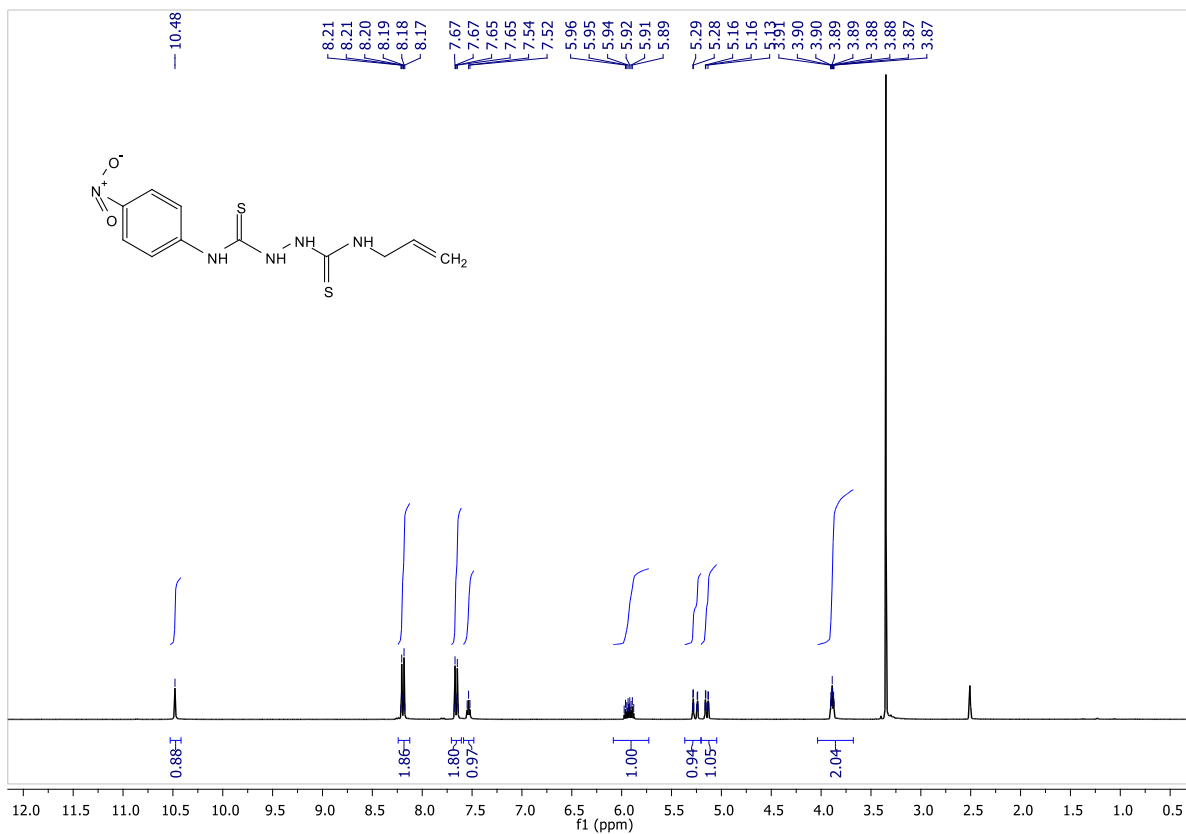


**Fig. S26.**  $^1\text{H-NMR}$  (400 MHz,  $\text{DMSO-}d_6$ ) spectra of compound **3g** ( $N^1$ -allyl- $N^2$ -(4-nitrophenyl)hydrazine-1,2-bis(carbothioamide)).

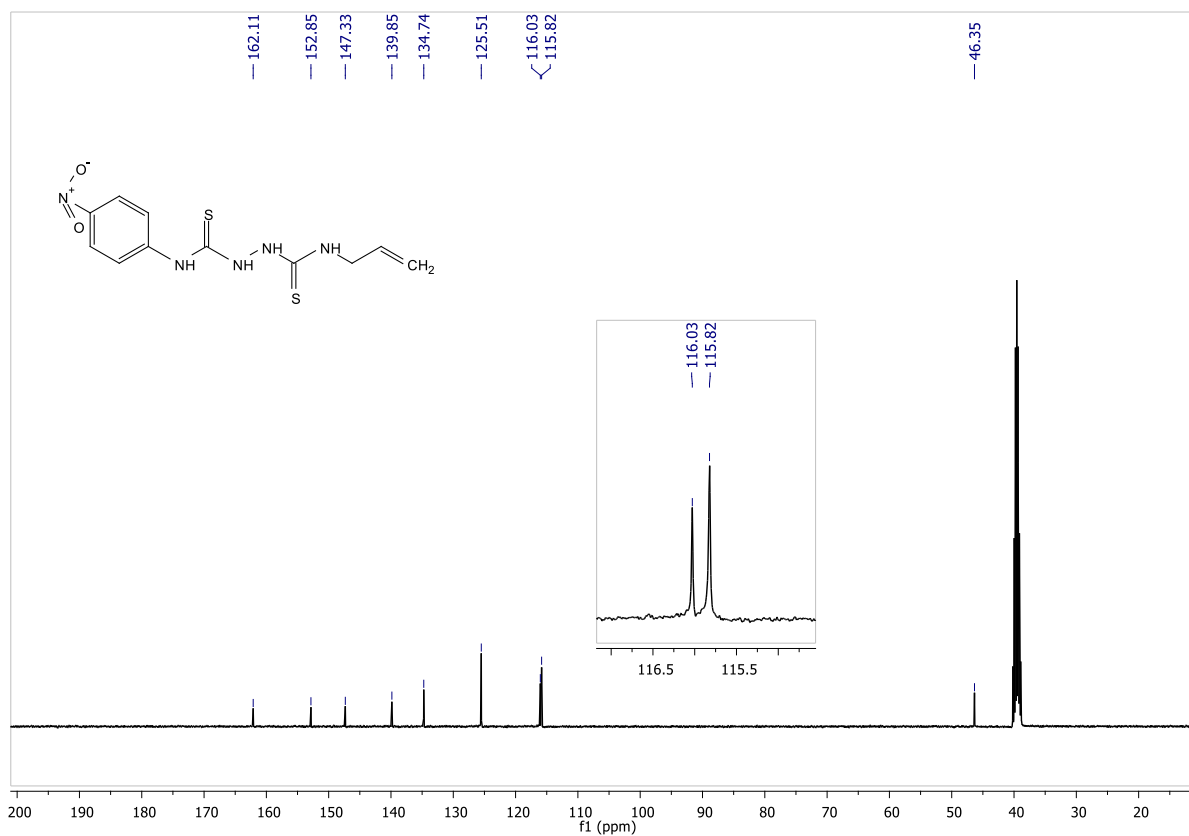


**Fig. S27.** <sup>13</sup>C-NMR (100 MHz, DMSO-*d*<sub>6</sub>) spectra of compound **3g** (*N*<sup>1</sup>-allyl-*N*<sup>2</sup>-(4-nitrophenyl)hydrazine-1,2-bis(carbothioamide)).

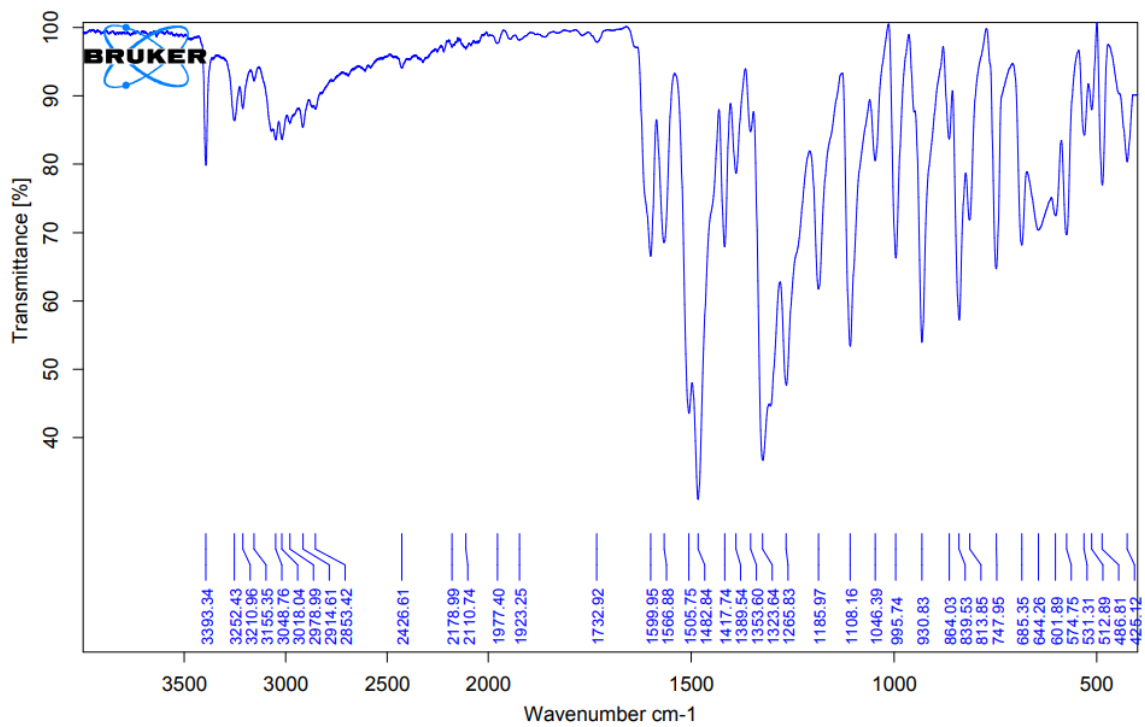
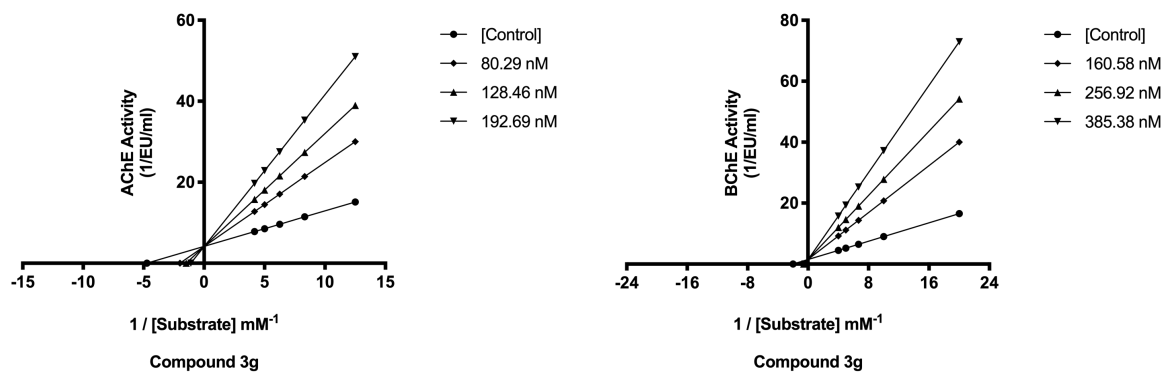
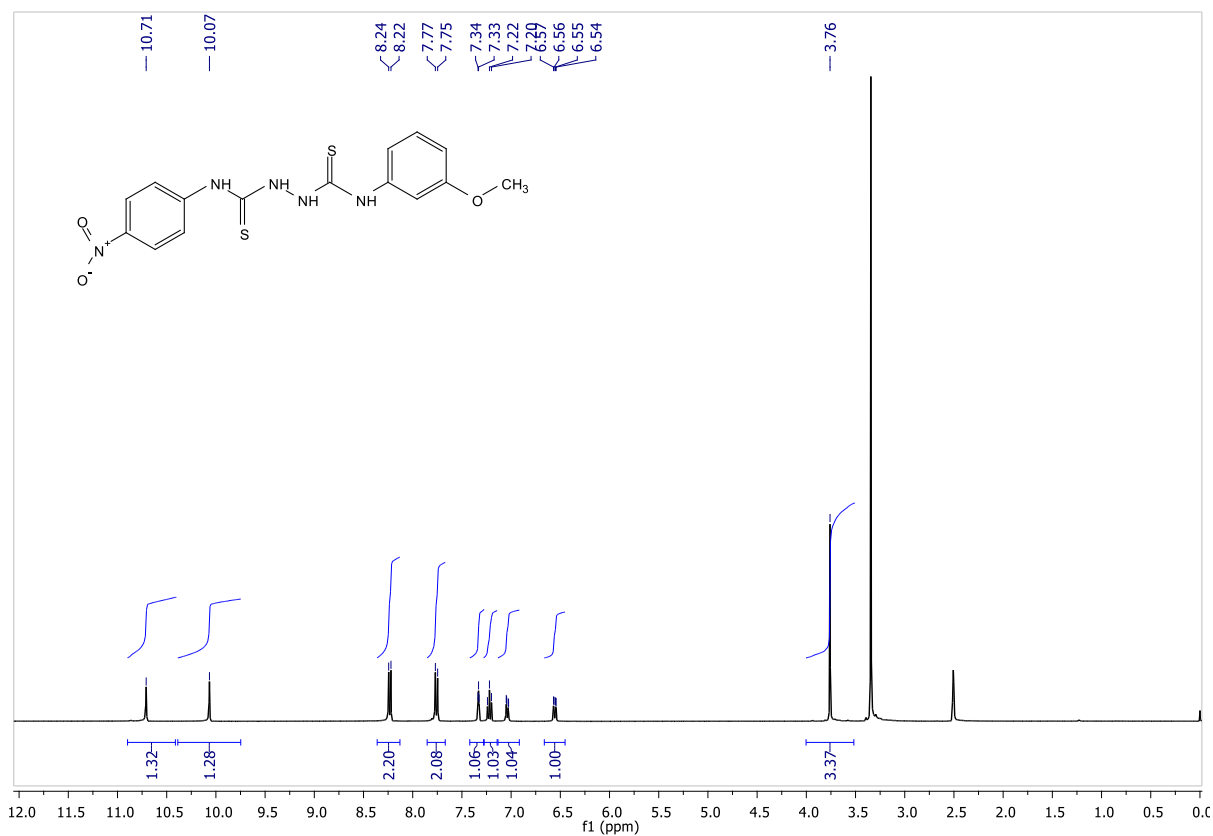


Fig. S28. FT-IR spectra of compound **3g** (*N*<sup>1</sup>-allyl-*N*<sup>2</sup>-(4-nitrophenyl)hydrazine-1,2-bis(carbothioamide)).



**Fig. S29.** Lineweaver-Burk plots of compound **3g** (*N*<sup>1</sup>-allyl-*N*<sup>2</sup>-(4-nitrophenyl)hydrazine-1,2-bis(carbothioamide)).



**Fig. S30.**  $^1\text{H-NMR}$  (400 MHz,  $\text{DMSO-}d_6$ ) spectra of compound **3h** ( $N^1$ -(3-methoxyphenyl)- $N^2$ -(4-nitrophenyl)hydrazine-1,2-bis(carbothioamide)).

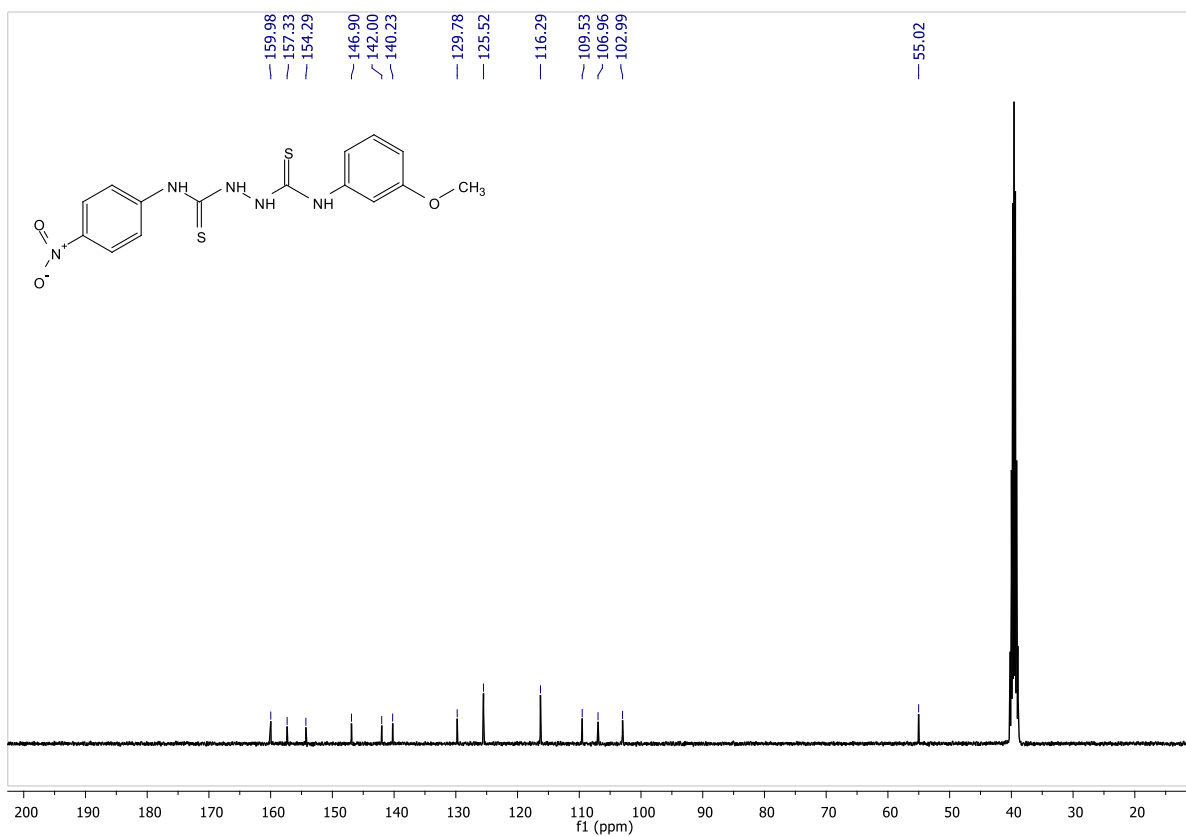


**Fig. S31.** <sup>13</sup>C-NMR (100 MHz, DMSO-*d*<sub>6</sub>) spectra of compound **3h** (*N*<sup>1</sup>-(3-methoxyphenyl)-*N*<sup>2</sup>-(4-nitrophenyl)hydrazine-1,2-bis(carbothioamide)).



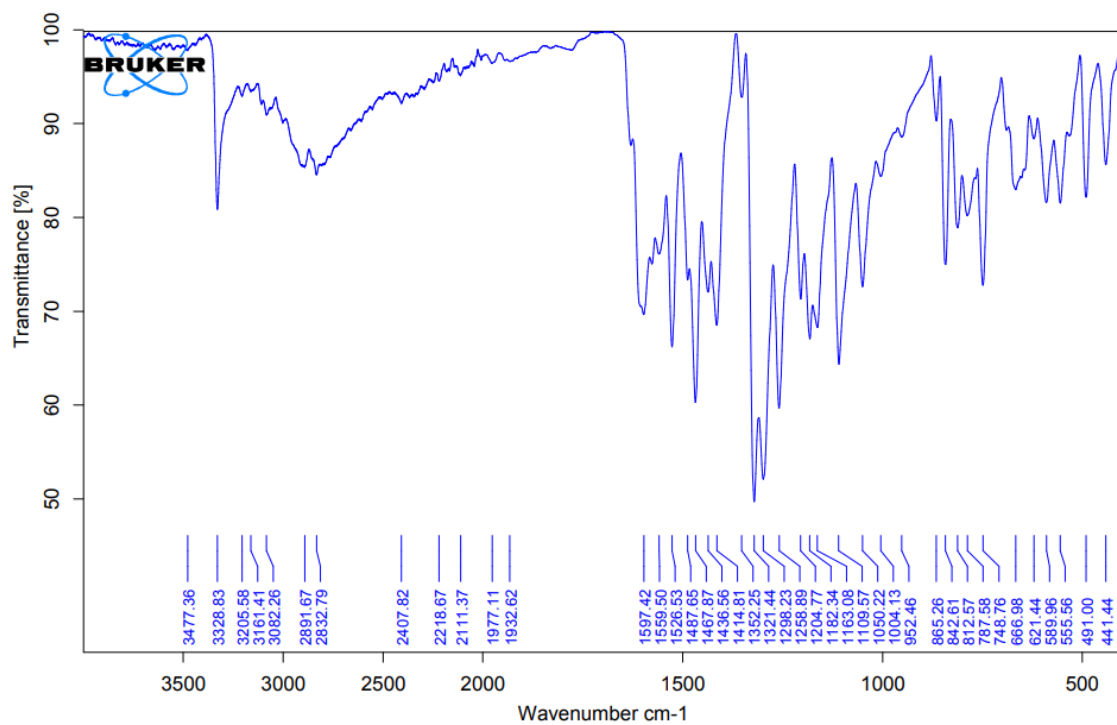


**Fig. S32.** FT-IR spectra of compound **3h** (*N*<sup>1</sup>-(3-methoxyphenyl)-*N*<sup>2</sup>-(4-nitrophenyl)hydrazine-1,2-bis(carbothioamide)).

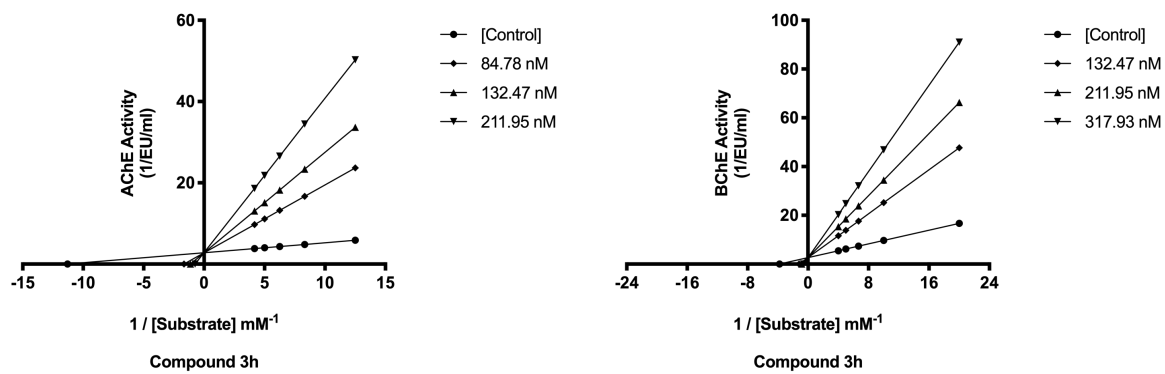


**Fig. S33.** Lineweaver-Burk plots of compound **3h** (*N*<sup>1</sup>-(3-methoxyphenyl)-*N*<sup>2</sup>-(4-nitrophenyl)hydrazine-1,2-bis(carbothioamide)).

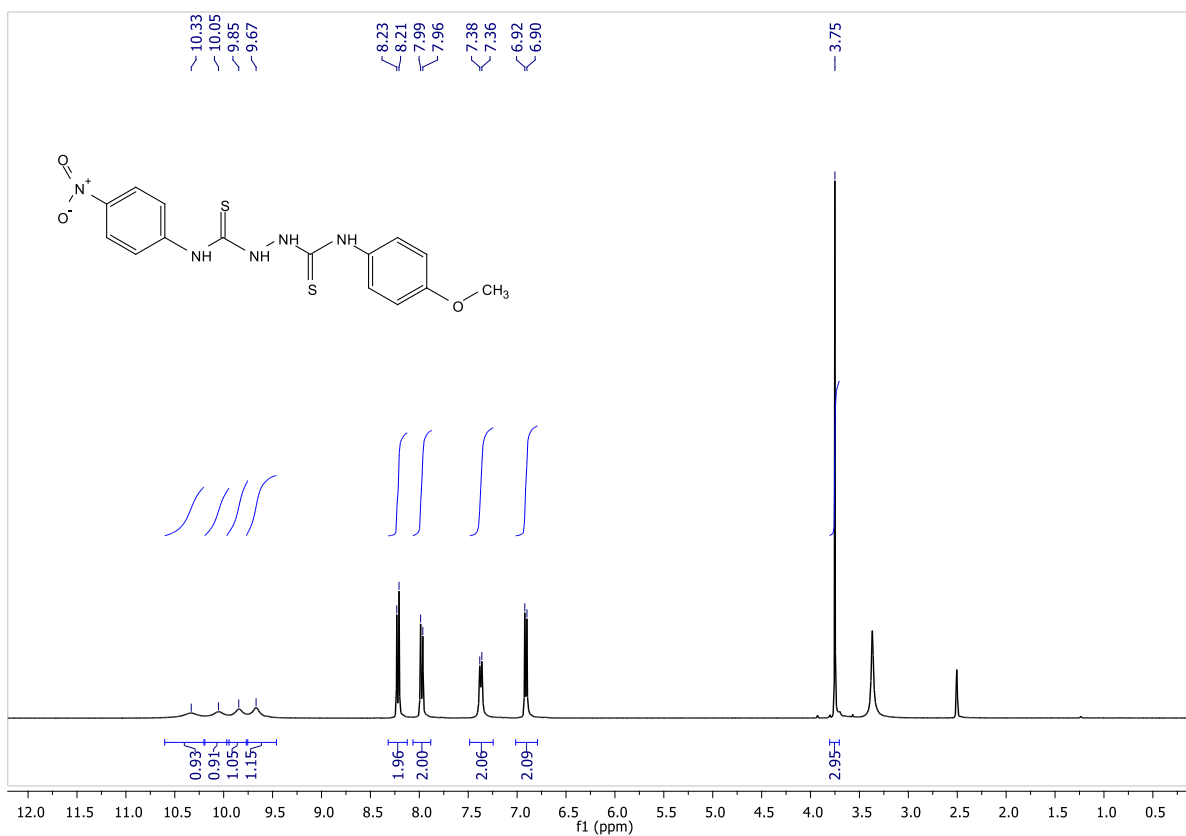


**Fig. S34.**  $^1\text{H-NMR}$  (400 MHz,  $\text{DMSO-d}_6$ ) spectra of compound **3i** ( $N^1$ -(4-methoxyphenyl)- $N^2$ -(4-nitrophenyl)hydrazine-1,2-bis(carbothioamide)).

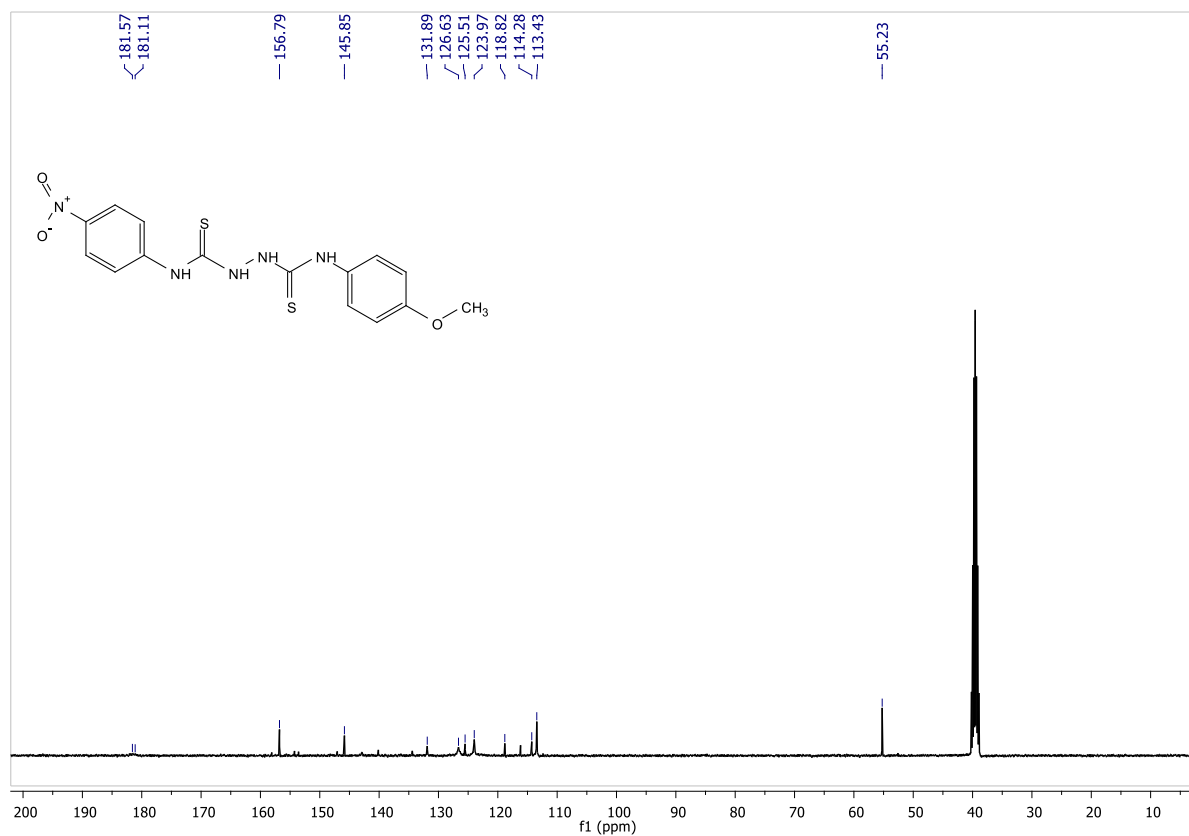


**Fig. S35.**  $^{13}\text{C}$ -NMR (100 MHz,  $\text{DMSO-}d_6$ ) spectra of compound **3i** ( $N^1$ -(4-methoxyphenyl)- $N^2$ -(4-nitrophenyl)hydrazine-1,2-bis(carbothioamide)).

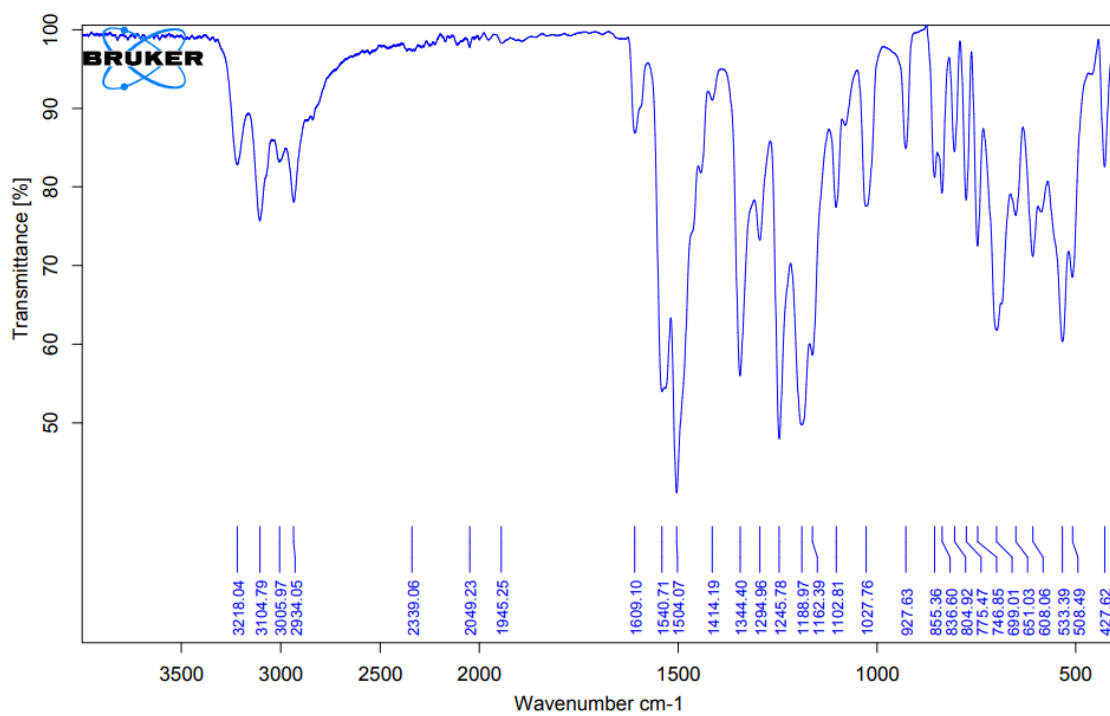


**Fig. S36.** FT-IR spectra of compound **3i** (*N*<sup>1</sup>-(4-methoxyphenyl)-*N*<sup>2</sup>-(4-nitrophenyl)hydrazine-1,2-bis(carbothioamide)).

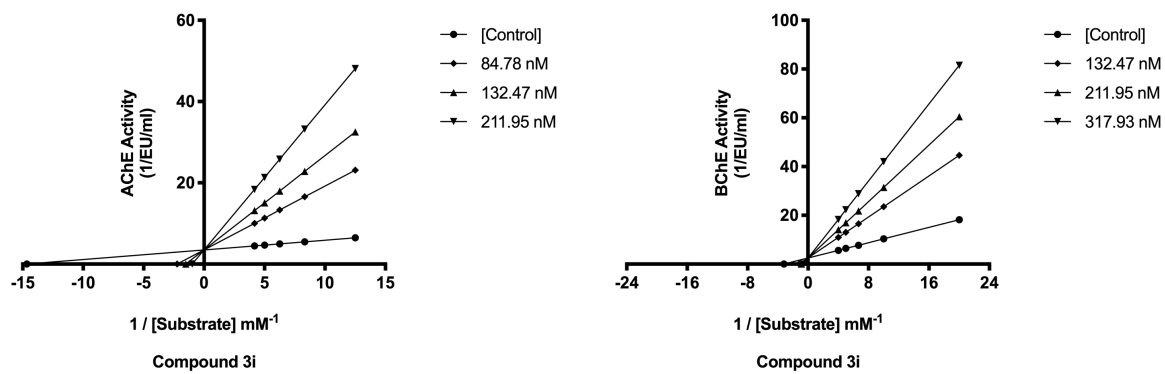


**Fig. S37.** Lineweaver-Burk plots of compound **3i** (*N*<sup>1</sup>-(4-methoxyphenyl)-*N*<sup>2</sup>-(4-nitrophenyl)hydrazine-1,2-bis(carbothioamide)).

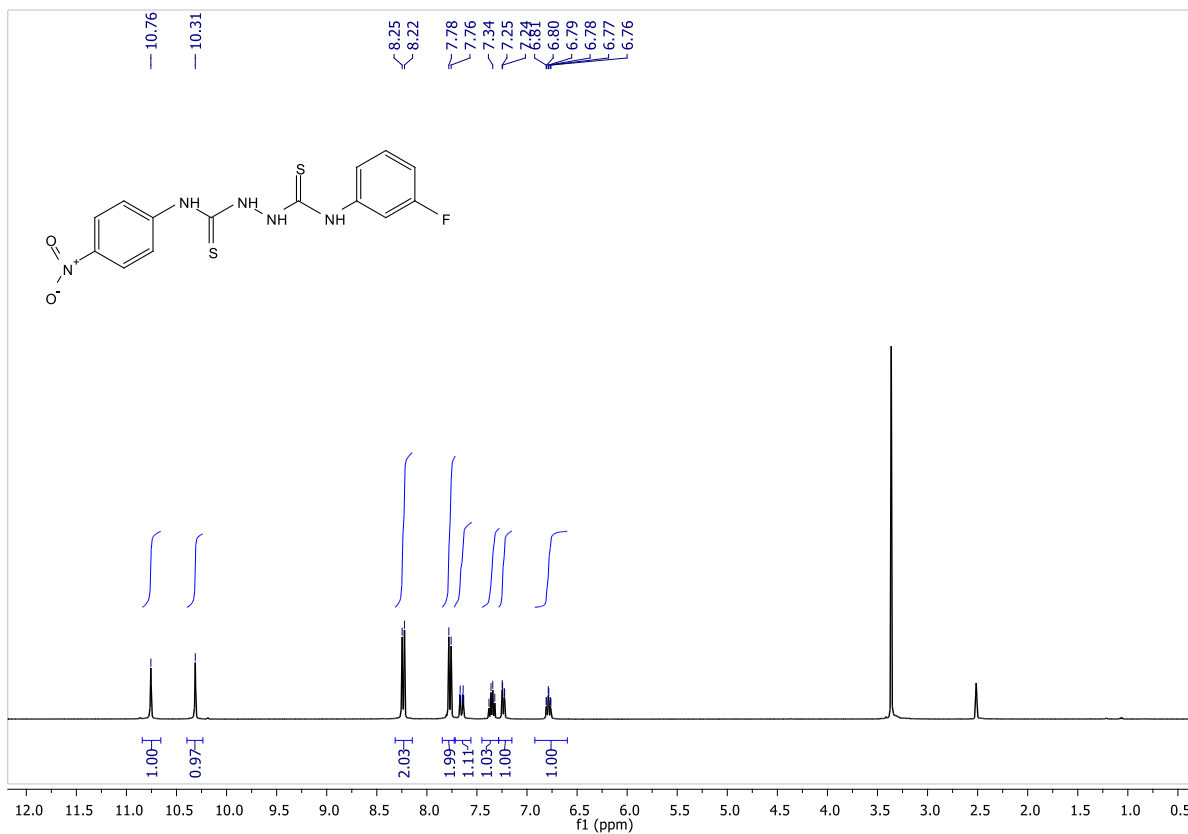


**Fig. S38.**  $^1\text{H-NMR}$  (400 MHz,  $\text{DMSO-}d_6$ ) spectra of compound **3j** ( $N^1$ -(3-fluorophenyl)- $N^2$ -(4-nitrophenyl)hydrazine-1,2-bis(carbothioamide)).

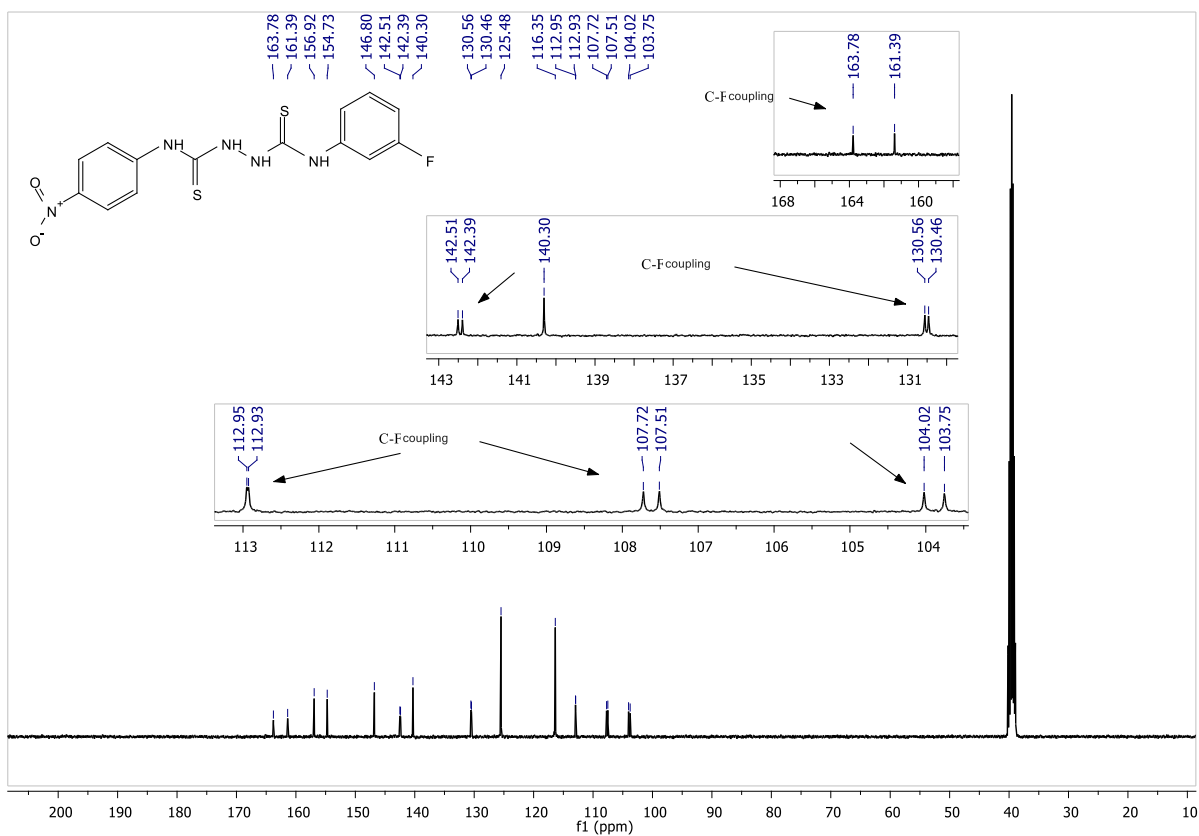


**Fig. S39.**  $^{13}\text{C}$ -NMR (100 MHz,  $\text{DMSO-}d_6$ ) spectra of compound **3j** ( $N^1$ -(3-fluorophenyl)- $N^2$ -(4-nitrophenyl)hydrazine-1,2-bis(carbothioamide)).



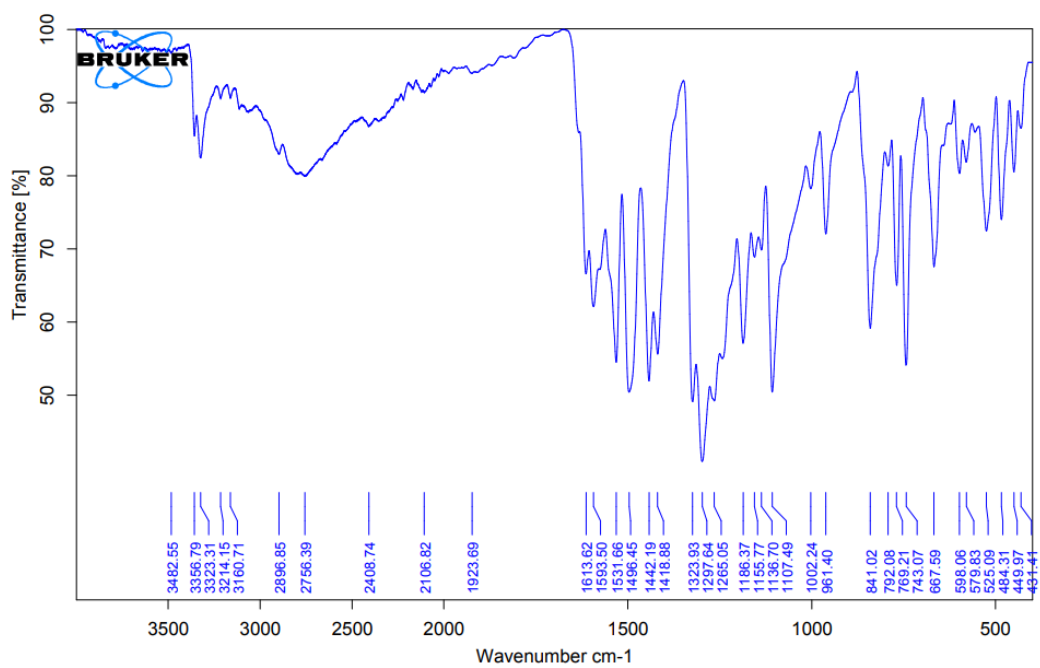


**Fig. S40.** FT-IR spectra of compound **3j** (*N*<sup>1</sup>-(3-fluorophenyl)-*N*<sup>2</sup>-(4-nitrophenyl)hydrazine-1,2-bis(carbothioamide)).

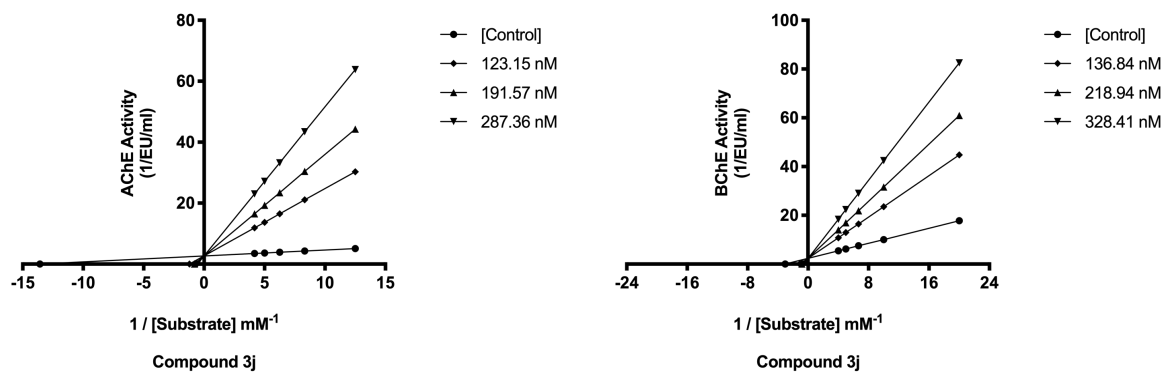


**Fig. S41.** Lineweaver-Burk plots of compound **3j** (*N*<sup>1</sup>-(3-fluorophenyl)-*N*<sup>2</sup>-(4-nitrophenyl)hydrazine-1,2-bis(carbothioamide)).

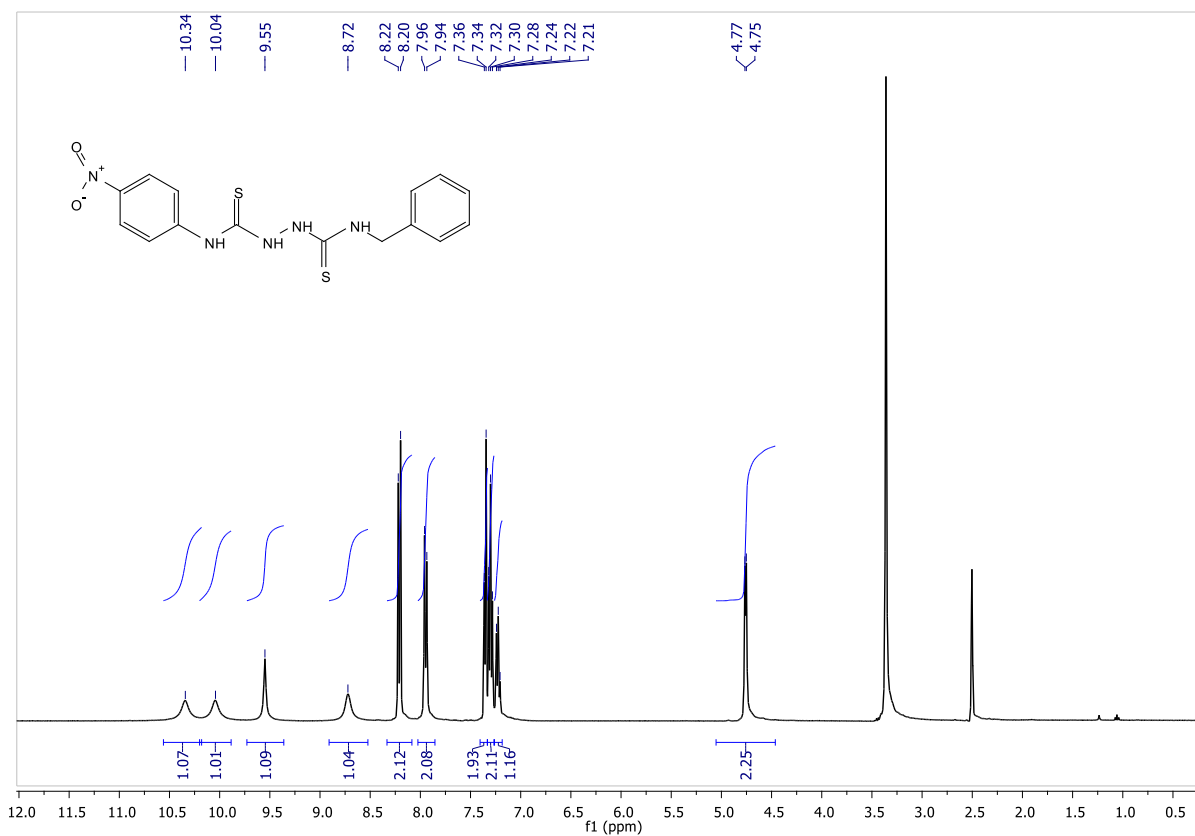


**Fig. S42.**  $^1\text{H-NMR}$  (400 MHz,  $\text{DMSO-}d_6$ ) spectra of compound **3k** ( $N^1$ -benzyl- $N^2$ -(4-nitrophenyl)hydrazine-1,2-bis(carbothioamide)).

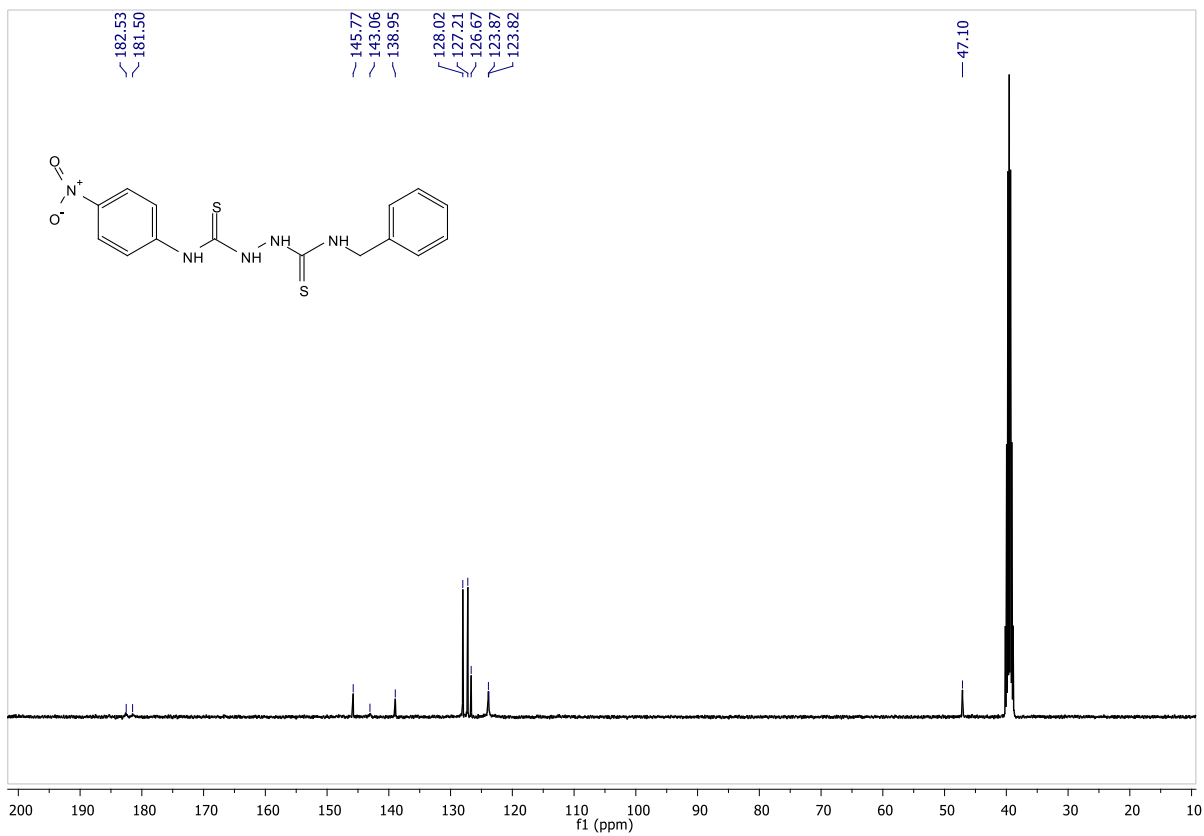


**Fig. S43.**  $^{13}\text{C}$ -NMR (100 MHz,  $\text{DMSO-}d_6$ ) spectra of compound **3k** ( $N^1$ -benzyl- $N^2$ -(4-nitrophenyl)hydrazine-1,2-bis(carbothioamide)).

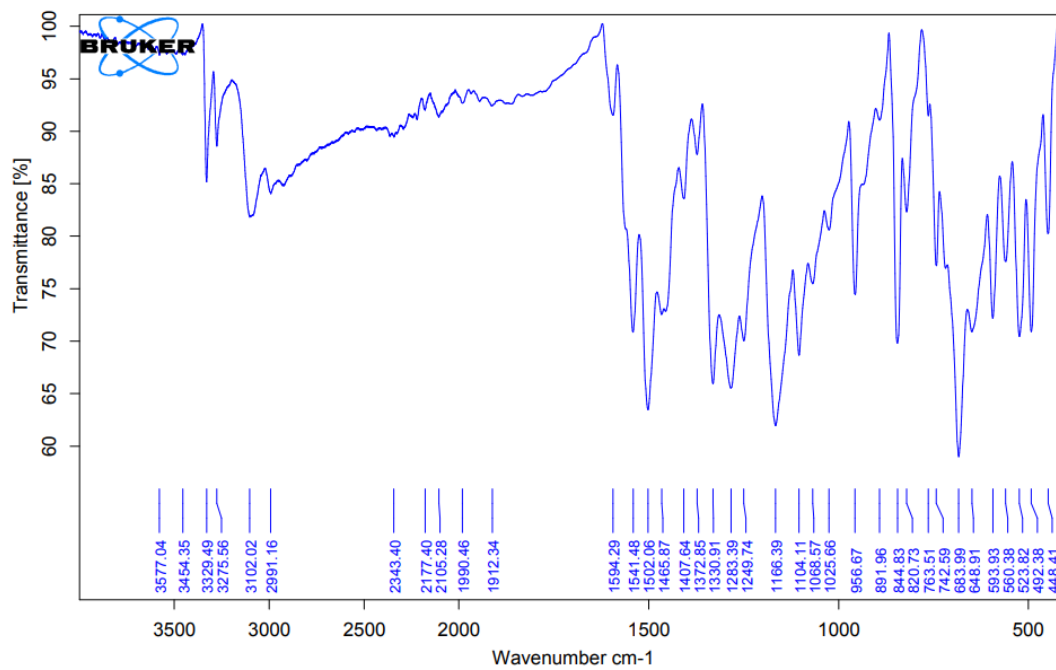
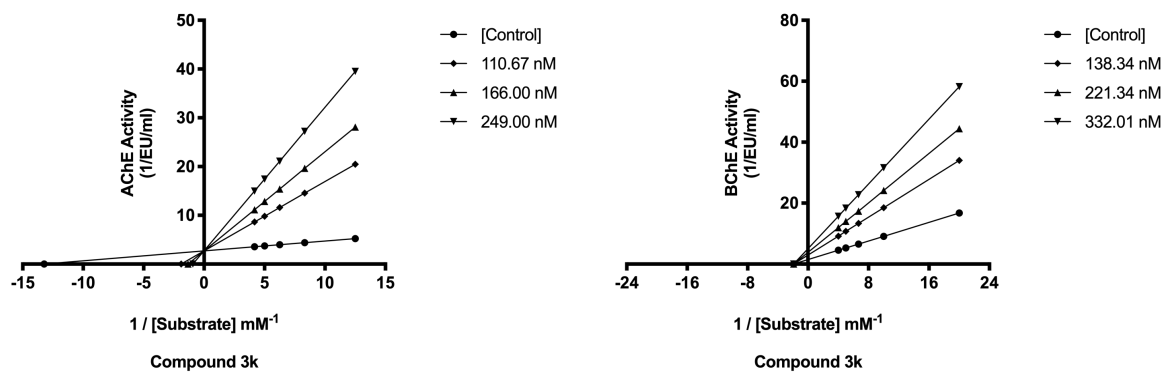
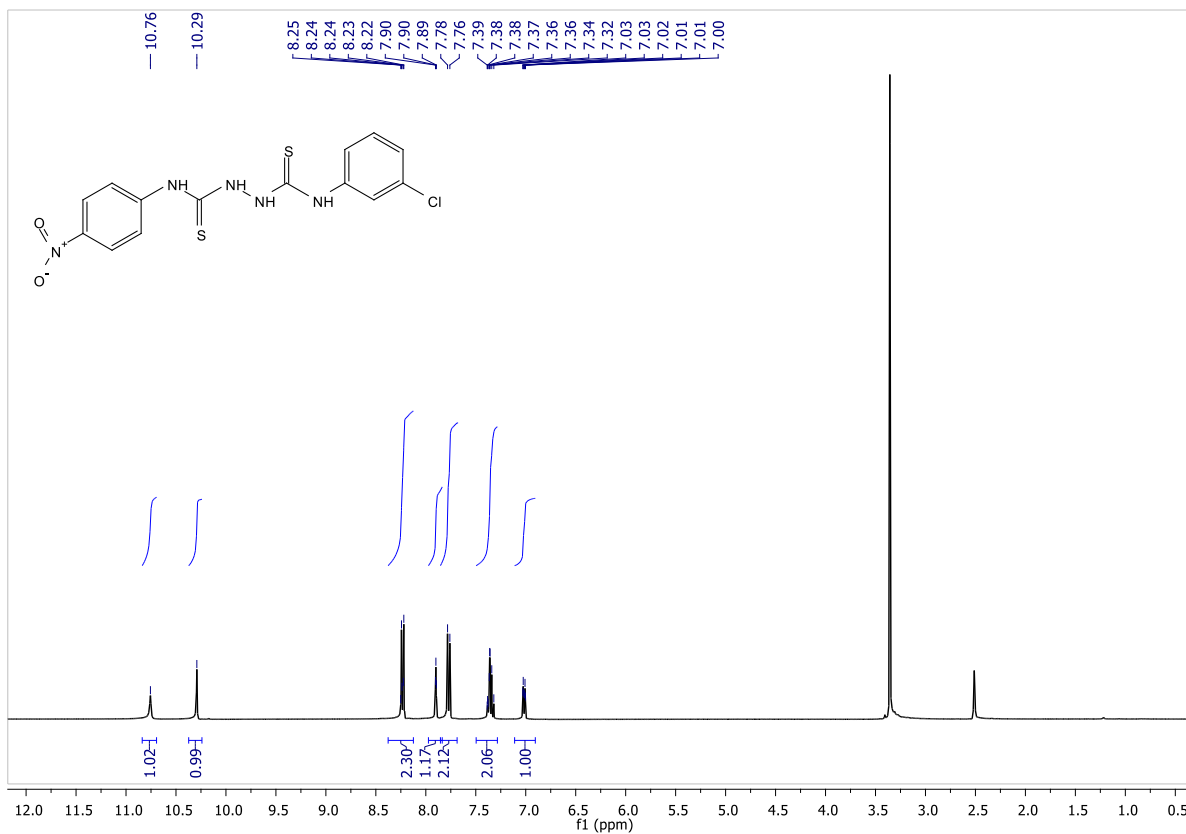


Fig. S44. FT-IR spectra of compound **3k** (*N*<sup>1</sup>-benzyl-*N*<sup>2</sup>-(4-nitrophenyl)hydrazine-1,2-bis(carbothioamide)).



**Fig. S45.** Lineweaver-Burk plots of compound **3k** (*N*<sup>1</sup>-benzyl-*N*<sup>2</sup>-(4-nitrophenyl)hydrazine-1,2-bis(carbothioamide)).



**Fig. S46.**  $^1\text{H-NMR}$  (400 MHz,  $\text{DMSO-}d_6$ ) spectra of compound **3I** ( $N^1$ -(3-chlorophenyl)- $N^2$ -(4-nitrophenyl)hydrazine-1,2-bis(carbothioamide)).

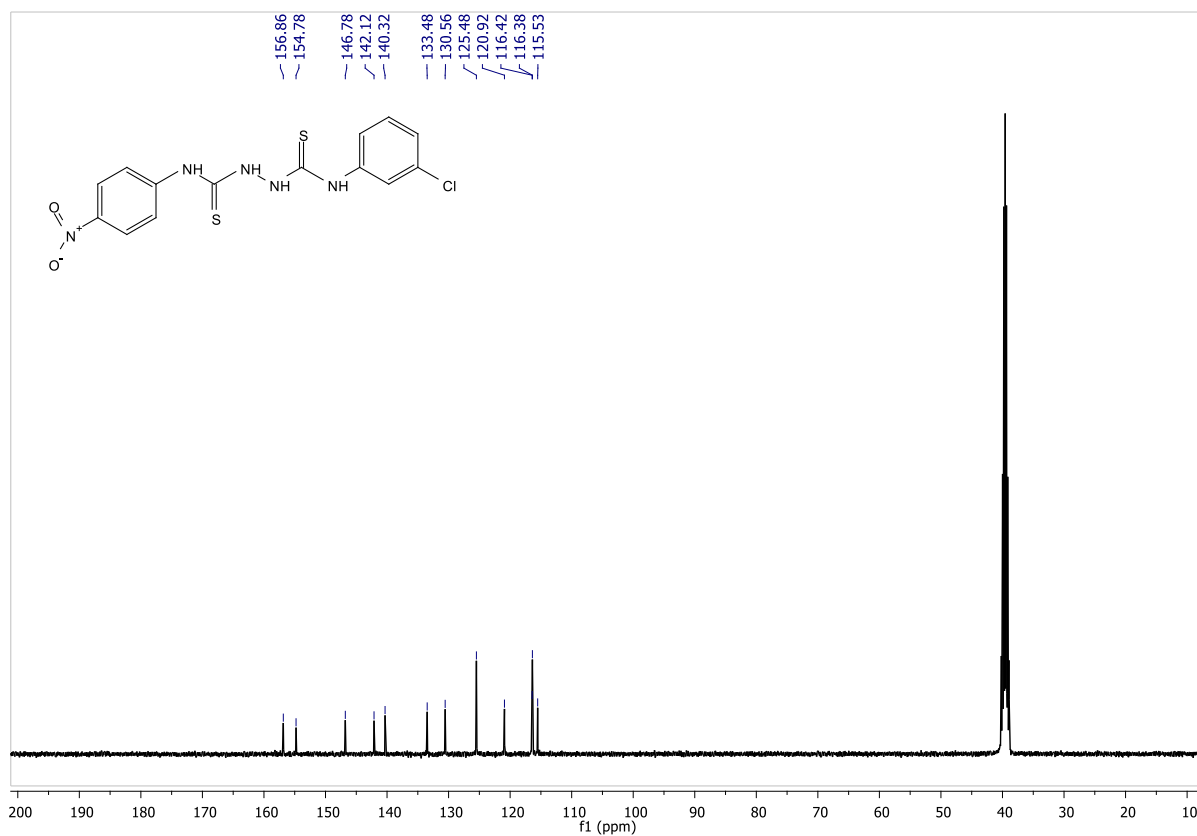


**Fig. S47.** <sup>13</sup>C-NMR (100 MHz, DMSO-*d*<sub>6</sub>) spectra of compound **3I** ( $N^1$ -(3-chlorophenyl)- $N^2$ -(4-nitrophenyl)hydrazine-1,2-bis(carbothioamide)).



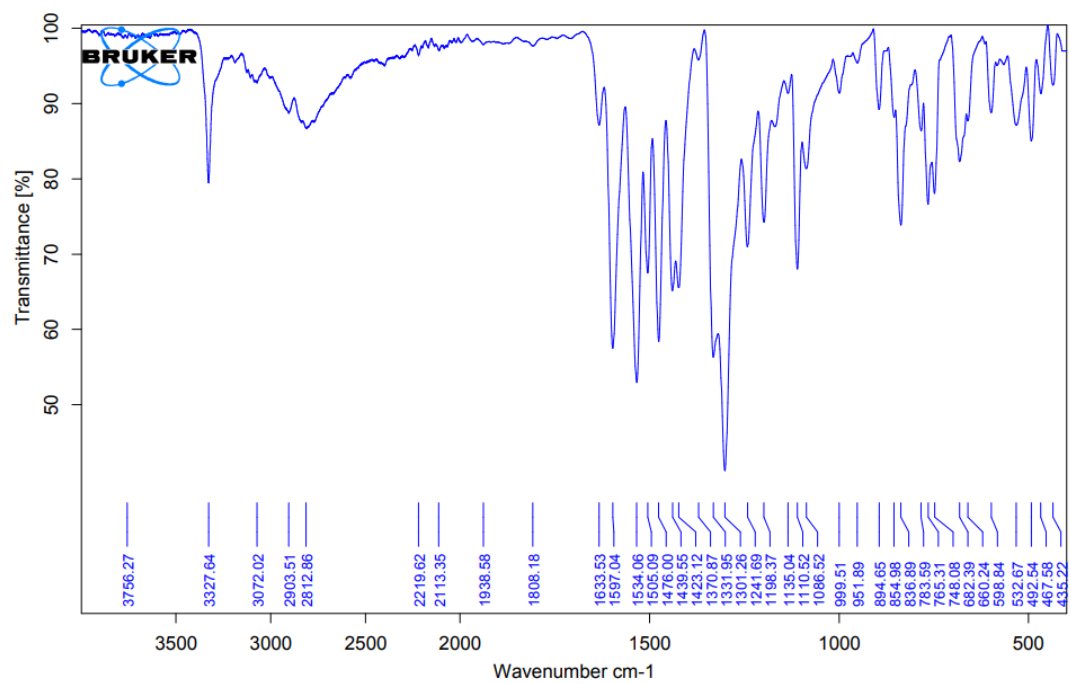


**Fig. S48.** FT-IR spectra of compound **3I** (*N*<sup>1</sup>-(3-chlorophenyl)-*N*<sup>2</sup>-(4-nitrophenyl)hydrazine-1,2-bis(carbothioamide)).

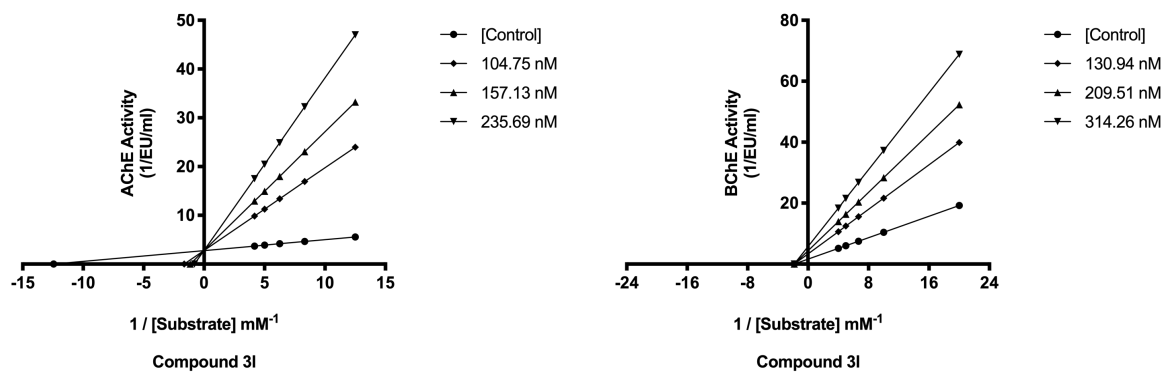


**Fig. S49.** Lineweaver-Burk plots of compound **31** (*N*<sup>1</sup>-(3-chlorophenyl)-*N*<sup>2</sup>-(4-nitrophenyl)hydrazine-1,2-bis(carbothioamide)).